FOREWORD

This report was prepared by the Engineering Mechanics Division of Battelle Memorial Institute under USAF Contract No. AF 33(616)-7257. This contract was initiated under Project No. 3044, "Aviation Lubricants", Task No. 30169, "Gas Turbine Lubricants". The work was administered under the direction of the Directorate of Materials and Processes, Aeronautical Systems Division, with Mr. K. L. Berkey and Mr. L. J. De Brohun, acting as project engineers.

This report covers work conducted from May 1, 1960, through February 28, 1961.

ABSTRACT

Lubrication processes at rolling contacts are being studied with a rolling-disk machine and X-ray system capable of measuring the dynamic oil-film thickness and deformation at rolling contacts. Data are presented for a refined engine oil (Reference Oil B), a white mineral oil, and a polyphenyl ether over extended ranges of operating conditions. The measured minimum film thickness at rolling contacts transverse to the rolling direction with these lubricants, having bulk viscosities ranging from 6 cp to over 500 cp, varied from 3 to 100 microinches under these conditions. For low-viscosity lubricants operating under moderate conditions of load, speed, and temperature, measured film thickness correlated well with elasto-hydrodynamic lubrication theory including both the elastic deformation of the contact surfaces and the increase in viscosity of the lubricant under pressure. Measured film thickness decreased significantly below theoretical under increasing load, speed, viscosity, and ambient temperature, at times by as much as a factor of 40.

Measurements of the elastic deformation at rolling contacts indicated that the contact stresses were less severe for conditions of low load and high speed and with high-viscosity lubricants. These deformation measurements also indicated less severe stresses, or more spreading of the lubricant pressures at the edges of the contacts, for those operating conditions under which the minimum film thickness increasingly deviated below theoretical.

It is proposed that, as the conditions of load, speed, and temperature at rolling contacts become more severe, flow properties of lubricants other than viscosity and pressure-viscosity become important in elastohydrodynamic lubrication. The data indicate that some form of reduced shear stress or "yielding" may occur in the high-pressure lubricant film at rolling contacts under these conditions. The Ree-Eyring theory for describing this type of non-Newtonian flow behavior of lubricants under pressure was used in developing a new theory of rolling-contact lubrication which predicts reductions in film thickness similar to those measured. Equipment and techniques are being developed for measuring these non-Newtonian properties of lubricants, which apparently depend on molecular structure.

This report has been reviewed and is approved.

R. L. ADAMCZAK
Asst Chief, Fuels and Lubricants Branch
Nonmetallic Materials Laboratory
Directorate of Materials & Processes

TABLE OF CONTENTS

LIST OF TABLES

TABLE

LIST OF FIGURES

FIGURE

LIST OF FIGURES
(Continued)

LIST OF FIGURES
(Continued)

STUDY OF THE EFFECT OF LUBRICANTS ON HIGH-SPEED ROLLING-CONTACT BEARING PERFORMANCE

INTRODUCTION

The lubrication of rolling-contact surfaces is important in many aircraft and missile systems. Machine elements such as rolling-element bearings and gears in these systems must operate reliably under severe conditions of load, speed, temperature, and in some cases, meager lubrication. In order to devise criteria for the development of improved lubricants and lubrication methods, a comprehensive study of the special type of lubrication which occurs at rolling contacts was undertaken.

In the early phases of this program, it was demonstrated that continuous lubricant films were generated in ball bearings and between colliding surfaces under many practical conditions[1]*. It appeared that hydrodynamic concepts could be used to describe rolling-contact lubrication if such theories were modified to include the elastic deformation of the surfaces and the increase in viscosity of the lubricant under pressure. Thus, the performance of rolling contacts was thought to depend to a large extent on the viscous-flow characteristics of lubricants under the high transient pressures and shear rates in the very thin lubricant films that are generated in small rolling-contact regions[2].

In the recent phases of this research, an X-ray method for measuring the oil-film thickness and the deformation at the rolling contact in a rolling-disk machine was developed[3] and has been used to obtain considerable data on several different lubricants over substantial ranges of load, speed, and temperature. A high-pressure rheology machine was designed and constructed for shearing a small film of lubricant of known dimensions under high hydrostatic pressure and at shear rates and stresses approaching those in bearings. Lubricant rheology data are needed under these conditions in order to relate the flow properties of lubricants, as determined by composition and molecular structure, to rolling-contact lubrication performance.

Manuscript released by the authors on 16 August 1961 for publication as an ASD Technical Report.
*Numbers in parentheses refer to references on page 56.

EXPERIMENTAL AND THEORETICAL STUDIES

Rolling-Contact Apparatus

The rolling-disk machine was designed and constructed to measure lubricant-film thickness and contact-deformation shape under rolling-contact conditions simulating the ball-race contacts in a typical ball bearing. Essentially, this machine consists of two hardened bearing-steel rollers loaded together, each mounted separately and driven independently by an electric motor, as shown in Figure 1. A small collimated beam of high-energy monochromatic X-rays is directed at the contact between the rollers parallel to the flattened contact region. A suitable radiation detector measures the amount of this X-ray beam that penetrates the oil film between these rollers. The X-ray wavelength was selected to penetrate oils readily, but to be absorbed by the roller steel. Thus, the oil-film thickness can be calculated from the calibrated intensity of the beam.

In order for the contact between the rollers to simulate the ball-race contacts in a bearing, the rollers are finished with a slight crown or transverse radius so that the elliptical contact region is about eight times as wide in the axial direction as in the rolling direction. Thus, by traversing the rolling-disk machine across the narrow X-ray beam on ball-and-runner tracks, the trace of the detected X-ray intensity on a strip-chart recorder depicts the shape of the deformed contact region between the rollers. The disk machine and most of the associated equipment are shown in Figure 2.

Preliminary experiments were conducted previously in the disk machine with three white mineral oils, a diester-base lubricant, and a silicone at normal contact loads up to 820 pounds (180,000 psi maximum Hertz stress), rolling speeds up to 5200 fpm, and temperatures up to 165 F[3,4]. Since the operating conditions of aircraft and missile bearings are sometimes more severe than these, additional apparatus was designed and constructed for extending the range of operating conditions in the disk machine.

New Drive System

High-frequency 2-horsepower drive motors and the required alternator system were procured for increased torque and rolling speed at the disk rolling contacts. The rated torque available was increased from 2.3 to 15 in-lb and the maximum design speed from 7000 to 20,000 rpm on the 2.88-inch-diameter disks (equivalent to maximum bearing speeds of about 2.2×10^6 DN*). A high-frequency variable-speed power supply was obtained for continuous speed variation during operation, as shown in Figure 3. The

* DN is the bore diameter in millimeters times the shaft speed in revolutions per minute.

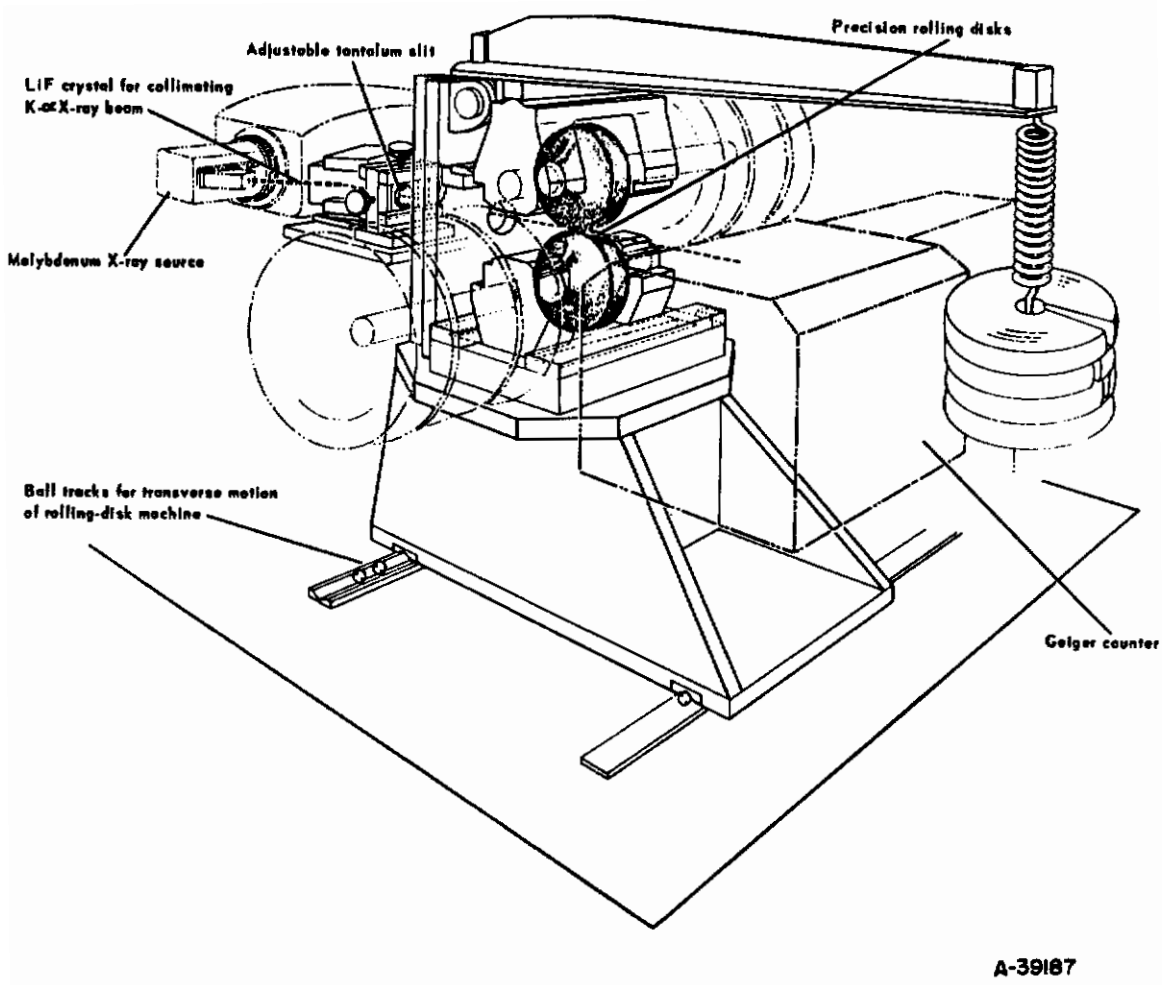

FIGURE 1. ROLLING-DISK MACHINE AND X-RAY SYSTEM FOR ROLLING-CONTACT-LUBRICATION EXPERIMENTS

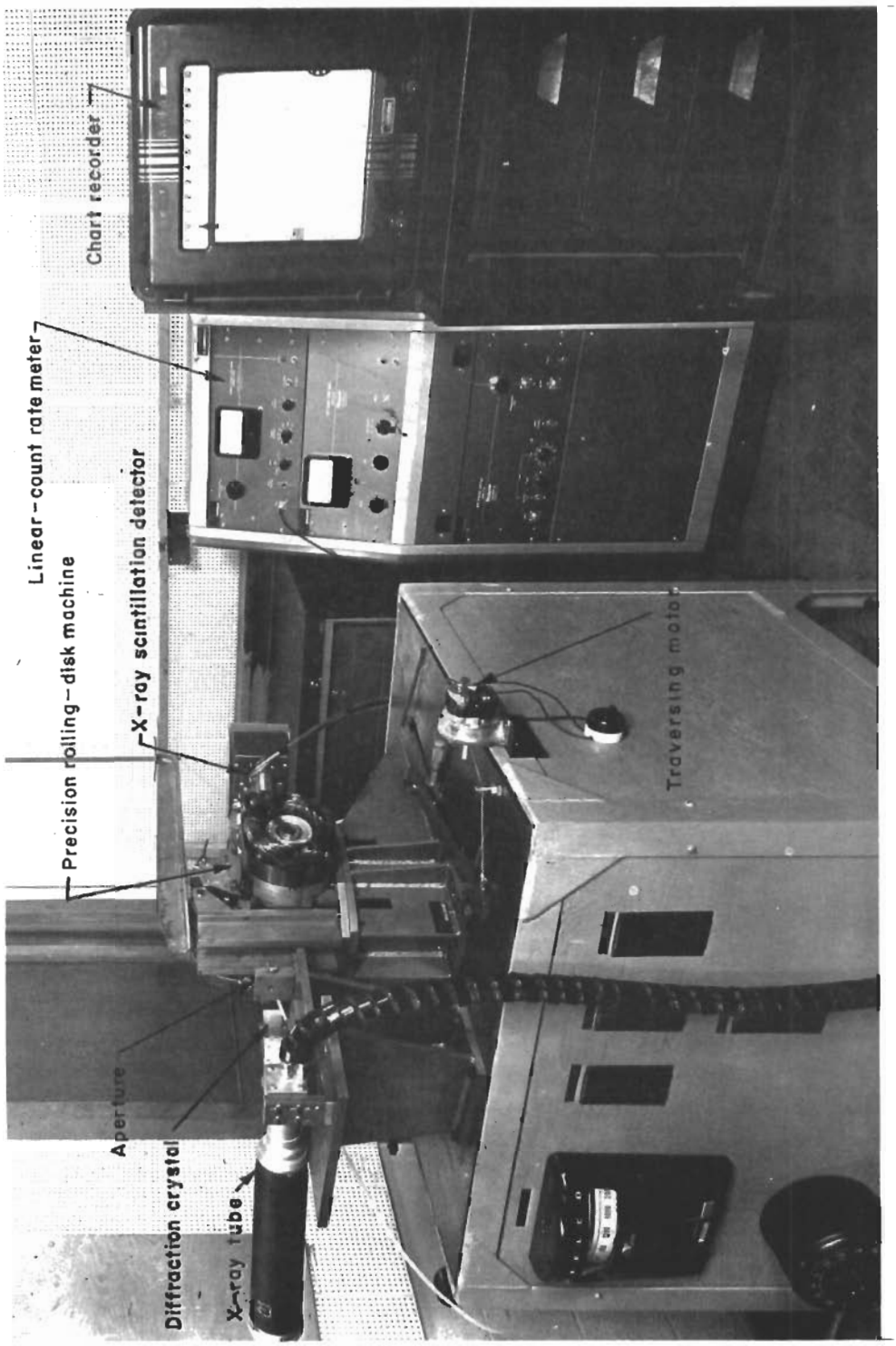

N72264

FIGURE 2. ROLLING-DISK MACHINE SHOWING X-RAY COUNTING EQUIPMENT

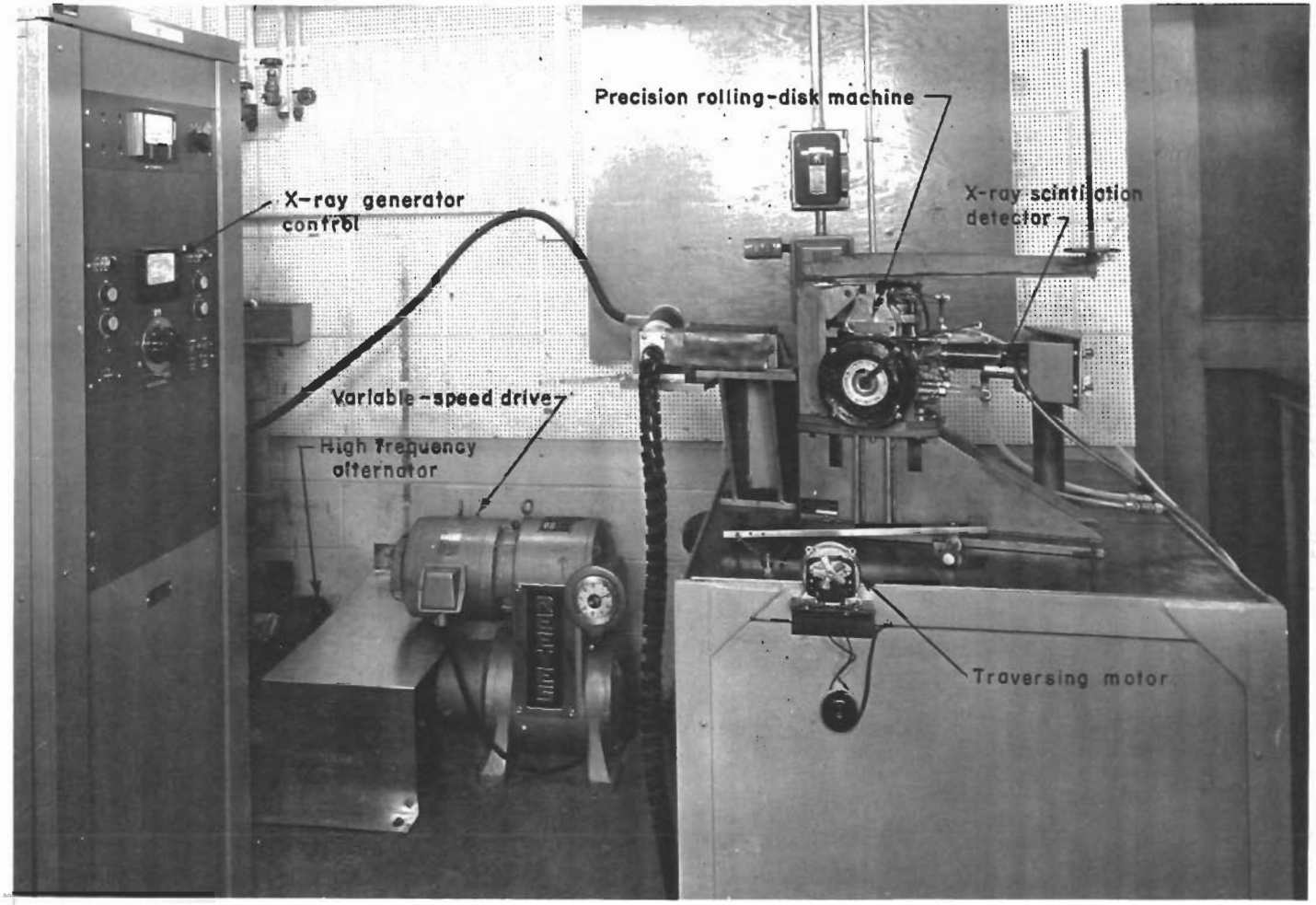

N72265

FIGURE 3. ROLLING-DISK MACHINE SHOWING X-RAY GENERATOR AND DRIVE-MOTOR ALTERNATOR

motors and alternator were installed, together with other new instrumentation and apparatus, on an auxiliary set of specially stabilized SAE 52100 steel disk rotors. With this increased drive torque, the load capacity of the machine was increased to 1600 (225,000 psi Hertz stress) pounds normal disk load, which is typical of the maximum ball-race loading in full-scale aircraft-engine bearings.

Disk-Heating System

Previous experimental and theoretical results have indicated that the important thermal parameter governing the film thickness in rolling-contact lubrication is the surface temperature of the rolling elements[3,5,6]. For high-temperature experiments, therefore, it is desirable that the disks be heated directly. Since the hot spots on radiation-type electrical heaters can cause excessive decomposition of test lubricants, an induction heating system was selected for direct heating of the disks.

Two induction coils were mounted on each rotor, one on each side of the roller or disk surface, as shown in Figure 4. These coils heat the rotor material directly, and the heat flows by conduction to the contacting surfaces of the disks. The metal temperature on these contacting surfaces was measured with a calibrated thermocouple mounted inside an open-end tube with both the thermocouple and the tube end held very near the disk surface. The tube around this thermocouple has its open end machined to match the contour of the disk, so that a slight suction of air from an aspirator through the tube and across the thermocouple provides the necessary sensitivity for this disk-temperature-sensing system. An immersion heater in the bypass line of the supply oil system is used to maintain the oil temperature approximately equal to the disk surface temperature.

The induction heating system was selected for its convenience and for its ability to heat the roller surfaces directly without inducing severe thermal gradients in the oil. It was found, however, that the induction heater induced excessive noise in the X-ray detector circuits (probably in the photomultiplier tube in the scintillation detector). Therefore, the system is operated intermittently at high temperatures so that the film thickness is measured only during those intervals when the induction heater is off. The variation in disk-surface temperature with this procedure was kept down to 1 or 2 F, which is not considered excessive.

Minimum Film-Thickness Measurements

With the rolling-disk machine modified as described above, the minimum film thickness was measured over most of the extended range of operating conditions with a white-mineral oil (135 SSU at 100 F), a highly refined aircraft engine oil base-stock (Reference Oil B, conforming to grade SAE 50),

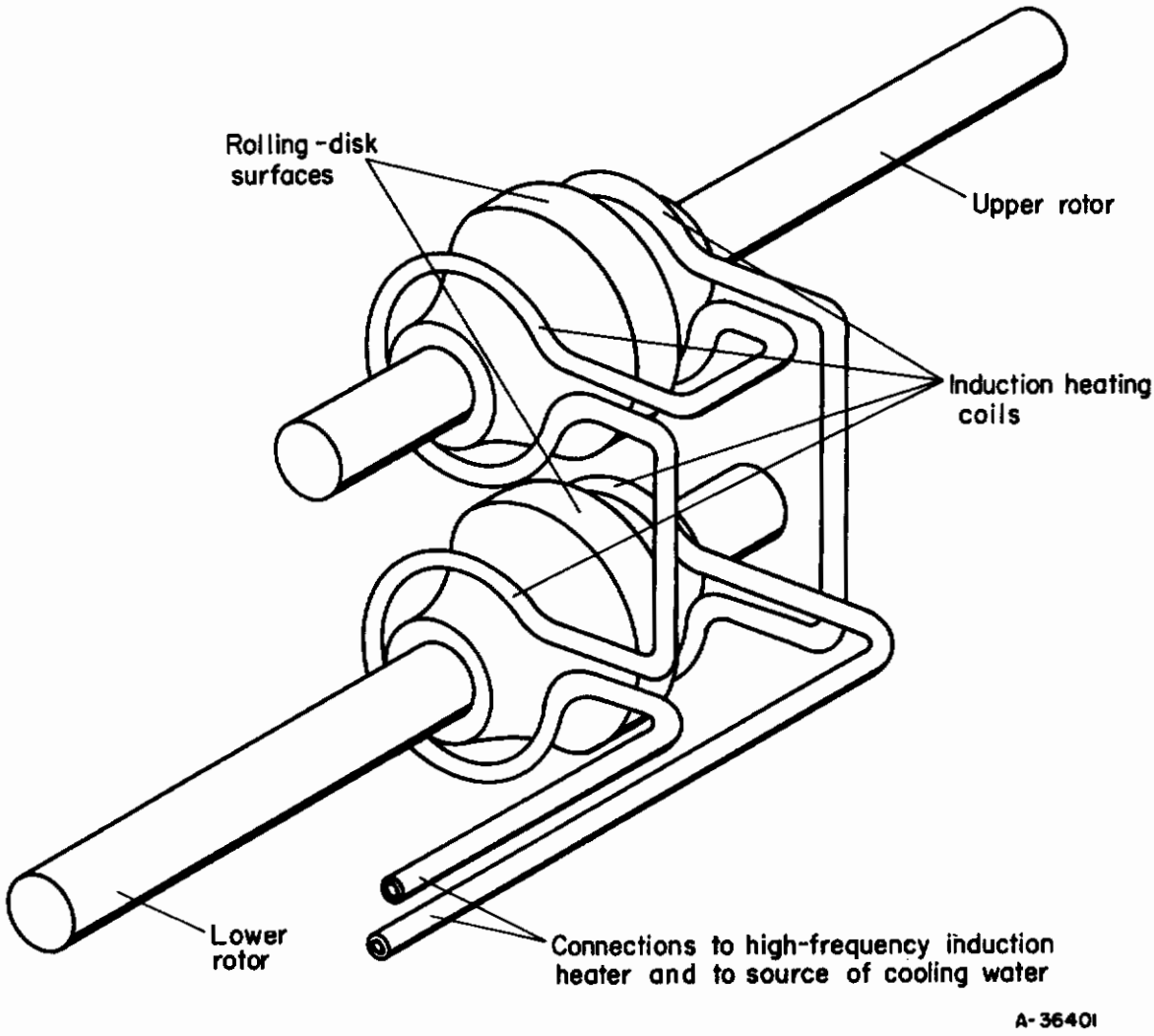

FIGURE 4. LOCATION OF HIGH-FREQUENCY INDUCTION COILS FOR HEATING THE ROLLING-DISK SURFACES

and a polyphenyl ether synthetic base stock. The viscosity and density of these lubricants at atmospheric pressure are given as a function of temperature in Figures 5 and 6. Data for a silicone and a diester lubricant, for which film-thickness data were obtained previously[3,4], are included in these figures for purposes of comparison. Average coefficients of pressure-viscosity* for these lubricants were calculated by fitting the best straight line on a semilog plot of viscosity versus pressure at constant temperature from the published ASME-Harvard data[7] for oils of similar composition and viscosity. The coefficients thus obtained are plotted in Figure 7. Since no pressure-viscosity data for polyphenyl ether were available, the coefficients for this lubricant plotted in Figure 7 and used in the analysis of the film-thickness data were estimated on the basis of available experimental data for highly aromatic and fused-ring hydrocarbons[7,8].

The minimum-film-thickness data from the rolling-disk machine are presented in Table 1, along with the calculated elasto-hydrodynamic dimensionless parameters for each point, based on the lubricant-properties data given in Figures 5, 6, and 7. These parameters are useful in obtaining a comparison of the data with available lubrication theories. Theories that have in the past been most successful in predicting the lubricant film thickness between rolling contacts combine both the elastic deformation of the bearing surfaces under the influence of the high contact pressures in the lubricant and the hydrodynamic flow of the lubricant in these contact regions, including the exponential increase of viscosity with pressure. Since this elastic deflection of the surfaces is often greater than the thickness of the film (which would not exist if the surfaces were rigid), this type of lubrication is known as elasto-hydrodynamic lubrication. Theories of elasto-hydrodynamic lubrication resulting in a formula for the film thickness at rolling contacts have been developed by Grubin[9] and Dowson and Higginson[10], including simultaneously the surface deformation and viscosity increase with pressure, and assuming an isothermal Newtonian lubricant. These theoretical formulas are as follows:

Grubin:
$$\frac{h_o}{R} = 1.13 \left(\frac{P'}{E'R}\right)^{-0.091} \left(\frac{\mu_o \gamma V}{R}\right)^{0.727} ,$$

Dowson and Higginson:
$$\frac{h_o}{R} = 0.972 \left(\frac{P'}{E'R}\right)^{-0.13} \left(\frac{\mu_o V}{E'R}\right)^{0.7} (\gamma E')^{0.6} ,$$

*The coefficient of pressure-viscosity γ is defined by the formula $\mu = \mu_o e^{\gamma p}$, where μ is the absolute viscosity at any pressure, μ_o is the viscosity at atmospheric pressure, and p is pressure.

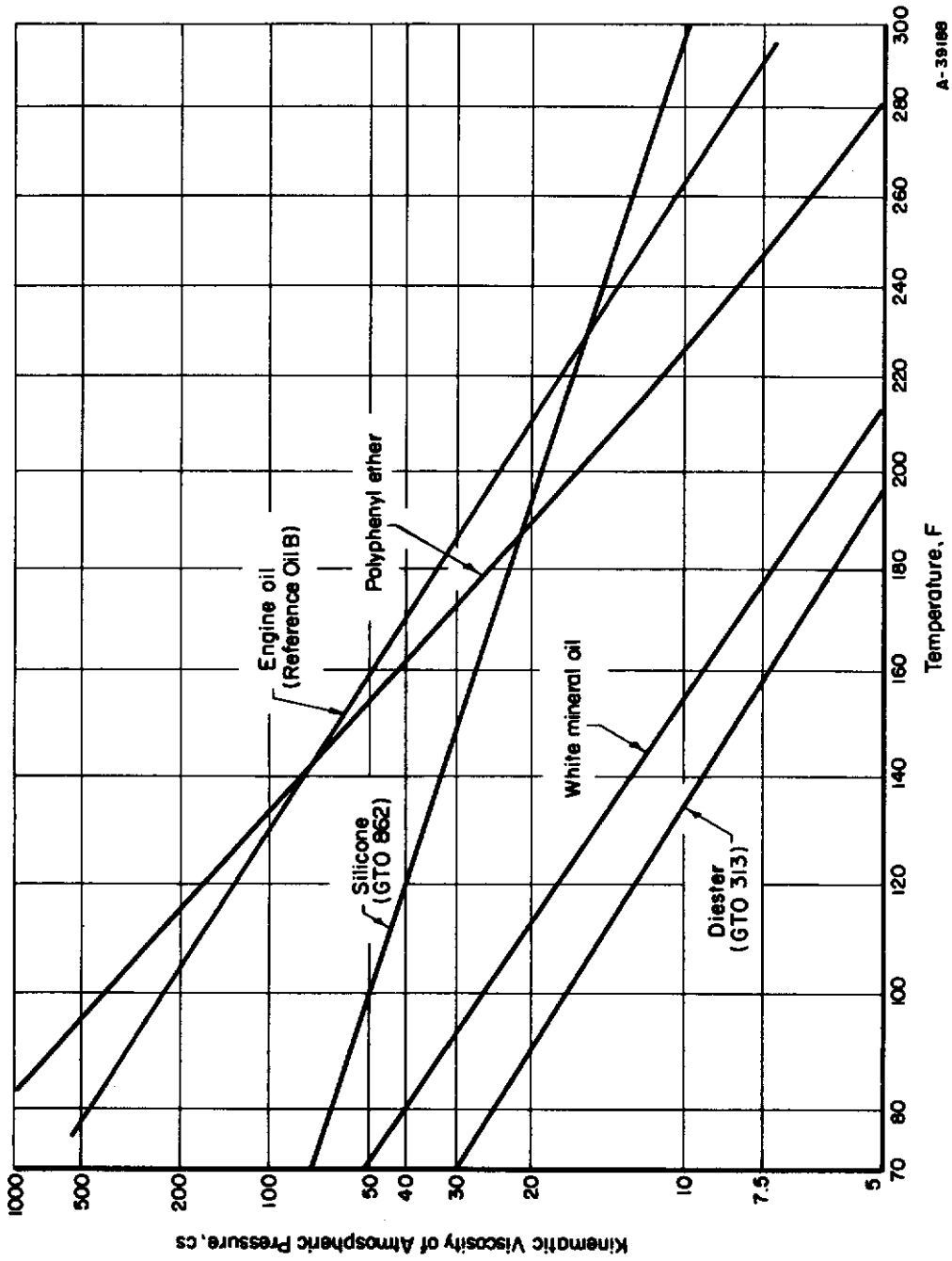

FIGURE 5. TEMPERATURE-VISCOSITY OF TEST LUBRICANTS

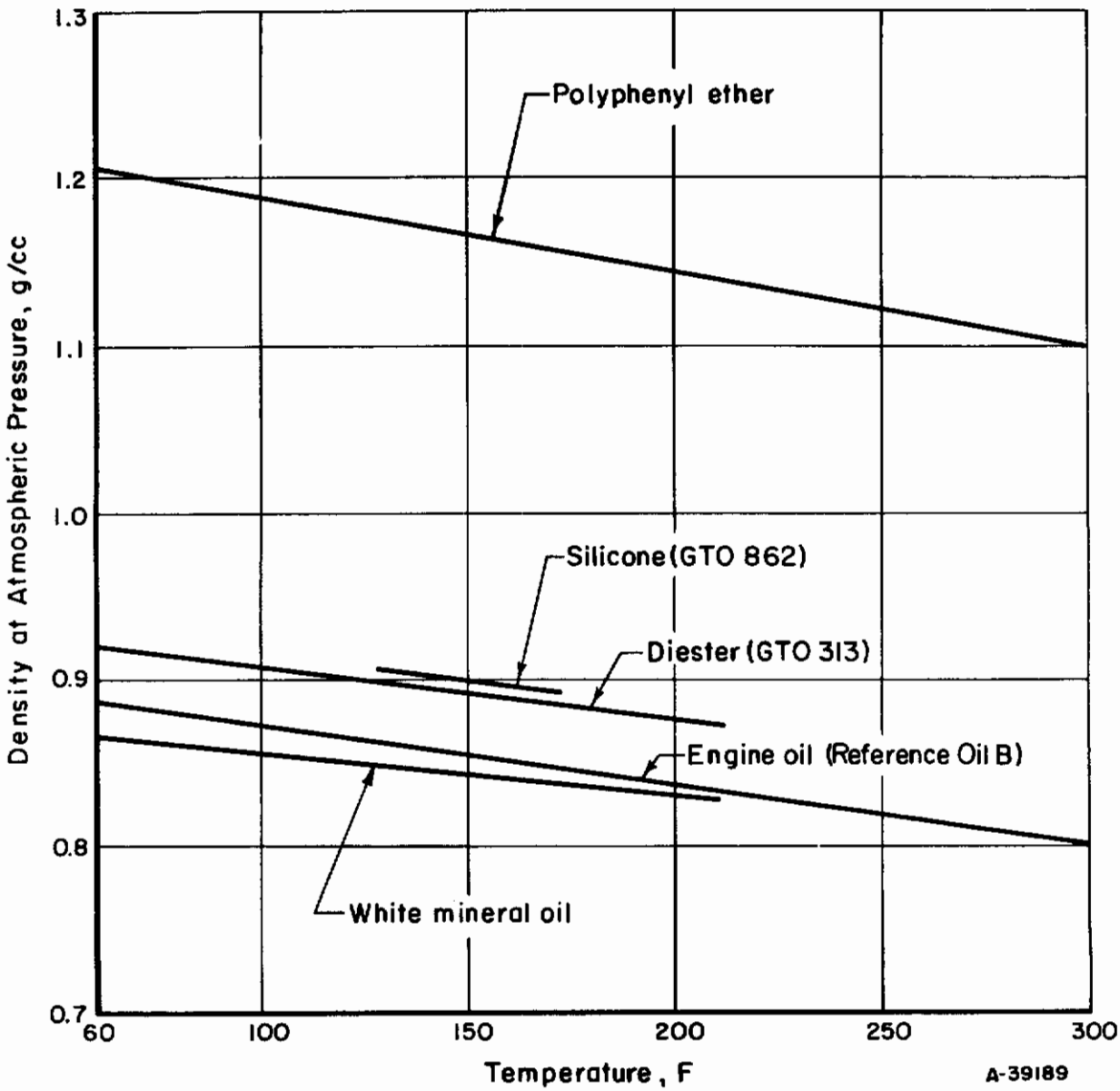

FIGURE 6. DENSITY OF TEST LUBRICANTS

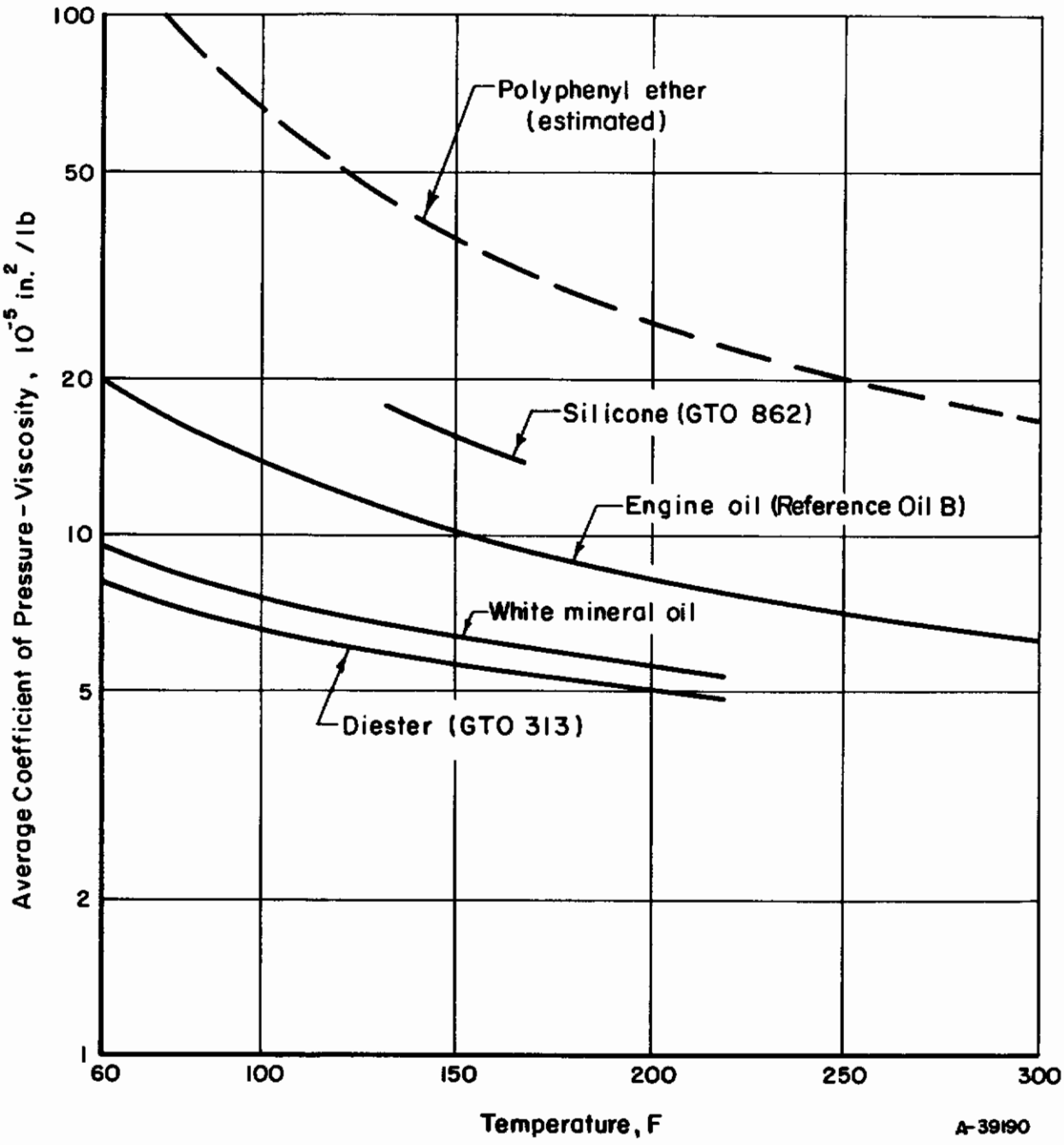

FIGURE 7. PRESSURE-VISCOSITY OF TEST LUBRICANTS

TABLE 1. LUBRICANT-FILM-THICKNESS DATA FROM THE ROLLING-DISK MACHINE

Transverse Disk Radius = 36 in.
R = 0.72 in., $E' = 5 \times 10^7$ psi

Lubricant	Disk Temperature, F	Viscosity at Disk Temperature, 10^{-7} lb-sec/in.^{2}	Rolling Speed, fpm	Load, lb	Minimum Film Thickness, 10^{-6} in.	Load Number, $\frac{p'}{E'R} \times 10^5$	Flow Number, $\frac{\mu_o \gamma V}{R} \times 10^8$	Film-Thickness Number, $\frac{h_o}{R} \times 10^6$
Engine oil	113	190	2600	535	32	9.8	518	44
(Ref. Oil B)	135	106	2600	85	42	2.9	218	58
	105	240	2600	535	35	9.8	740	49
	105	240	2600	235	42	5.6	740	58
	105	240	2600	85	47	2.9	740	65
	85	475	2600	235	60	5.6	1860	83
	90	384	2600	235	52	5.6	1407	72
	95	331	2600	535	45	9.8	1155	63
	95	331	2600	835	40	13.1	1155	56
	190	35	2600	235	17	5.6	43.0	24
	190	35	2600	535	11	9.8	43.0	15
	190	35	2600	835	7	13.1	43.0	10
	220	20	2600	385	11	7.9	22.7	15
	245	14	2600	385	6	7.9	14.2	8
	275	10	2600	385	3	7.9	9.0	4
	120	151	2600	385	30	7.9	369	42
	135	102	2600	235	37	5.6	218	51
	135	102	2600	535	25	9.8	218	35
	185	39	2600	235	14	5.6	49.1	19
	245	14	2600	17	25	0.98	14.2	35
	115	183	2600	235	37	5.6	471	51
	120	151	2600	535	22	9.8	369	31
White mineral oil	137	16.2	6900	85	19	2.9	41.6	26
	140	15.4	6900	235	13	5.6	39.0	18
	120	21.6	6900	85	32	2.9	58.8	44
	123	20.4	6900	235	18	5.6	54.7	25
	128	18.6	6900	235	16	5.6	49.2	22
	134	16.9	6900	235	15	5.6	44.0	21
	137	16.2	6900	235	14	5.6	41.6	19
	140	15.4	6900	235	14	5.6	39.0	19
	145	14.2	6900	235	14	5.6	35.4	19
	150	13.2	7500	235	14	5.6	35.2	19
	152	12.9	7500	235	14	5.6	34.4	19
	155	12.2	7500	235	14	5.6	32.0	19
	155	12.2	8300	235	16	5.6	35.5	22
	158	11.7	8300	235	15	5.6	33.5	21
	130	18.1	6400	85	26	2.9	44.4	36
	138	16.0	6400	235	14	5.6	38.1	19
	156	12.1	6400	235	8	5.6	27.1	12
	164	10.7	6400	235	7	5.6	23.2	10
	171	9.9	6400	235	6	5.6	21.1	8
	182	8.5	6400	235	5	5.6	17.5	7
	180	8.7	7200	235	7	5.6	20.5	10
	182	8.5	7200	235	6	5.6	19.7	8
	177	9.0	7200	235	7	5.6	21.2	10
	164	10.7	7200	235	10	5.6	26.1	14
	175	9.4	7200	235	7	5.6	22.5	10
	173	9.6	7200	235	8	5.6	23.0	12
	170	10.0	7200	235	9	5.6	24.0	13
	168	10.2	7200	235	10	5.6	24.9	14
	171	9.9	7200	235	9	5.6	23.7	13
	175	9.4	7200	235	7	5.6	22.5	10
	175	9.4	7900	235	8	5.6	24.8	12
	185	8.2	7900	235	6	5.6	20.9	8
	184	8.4	7900	235	7	5.6	21.4	10

TABLE 1. (Continued)

Lubricant	Disk Temperature, F	Viscosity at Disk Temperature, 10^{-7} lb-sec/in.^{2}	Rolling Speed, fpm	Load, lb	Minimum Film Thickness, 10^{-6} in.	Load Number, $\frac{P'}{E'R} \times 10^5$	Flow Number, $\frac{\mu_o VV}{R} \times 10^8$	Film-Thickness Number, $\frac{h_o}{R} \times 10^6$
White mineral oil	173	9.6	7900	235	9	5.6	25.3	13
	162	11.1	7900	235	11	5.6	30.2	15
	177	9.0	7900	235	8	5.6	23.3	12
	176	9.2	8700	235	10	5.6	26.2	14
	170	10.0	8700	235	12	5.6	29.0	17
	175	9.4	8700	235	10	5.6	27.2	14
	180	8.7	8700	235	9	5.6	24.8	13
	177	9.0	8700	235	9	5.6	25.7	13
	173	9.6	8700	235	12	5.6	27.8	17
	174	9.5	8700	385	8	7.9	27.5	12
	176	9.2	8700	535	7	9.8	26.2	10
	175	9.4	8700	535	6	9.8	27.2	8
	170	10.0	8700	535	8	9.8	29.0	12
	128	18.6	6800	17	62	0.98	48.5	86
Polyphenyl ether	136	151	6800	17	67	0.98	2510	93
	161	69	6800	17	60	0.98	886	83
	163	64	6800	85	37	2.9	822	51
	167	57	6800	235	27	5.6	710	38
	169	54	6800	235	27	5.6	653	38
	169	54	6800	235	26	5.6	653	36
	169	54	6800	235	26	5.6	653	36
	155	81	6800	17	67	0.98	1101	93
	165	61	7500	235	27	5.6	839	38
	172	50	8300	235	26	5.6	715	36
	172	50	7500	235	25	5.6	646	35
	172	50	6800	235	24	5.6	586	33
	124	235	6900	85	69	2.9	4510	96
	137	144	6900	235	42	5.6	2370	58
	146	108	6900	235	37	5.6	1655	51
	143	119	6900	535	30	9.8	1870	42
	150	95	6900	535	25	9.8	1383	35
	155	81	6900	535	22	9.8	1118	31
	160	69	6900	535	20	9.8	899	28
	160	69	6900	235	27	5.6	899	38
	117	308	6900	85	98	2.9	6490	136
	140	131	6900	535	30	9.8	2110	42
	150	95	6900	535	24	9.8	1383	33
	155	81	6900	535	22	9.8	1118	31
	156	79	6900	535	22	9.8	1090	31
	136	151	6900	235	49	5.6	2550	68
	142	124	6900	235	45	5.6	1950	63
	145	110	6900	235	43	5.6	1687	60
	148	102	6900	235	39	5.6	1525	54
	152	89	6900	235	35	5.6	1262	49
	158	74	6900	235	31	5.6	993	43
	166	59	6900	235	27	5.6	746	38
	178	44	6900	235	22	5.6	506	31
	179	42	6900	235	22	5.6	483	31
	181	40	6900	235	21	5.6	445	29
	191	35	6900	235	18	5.6	362	25
	210	22	6900	235	13	5.6	203	18
	217	19	6900	235	11	5.6	167	15
	146	108	6900	235	37	5.6	1655	51
	155	81	6900	535	22	9.8	1118	31
	163	64	6900	835	13	13.1	834	18
	165	61	6900	1135	10	16.1	771	14
	167	57	6900	1210	8	16.8	699	11

where h_o is the minimum film thickness, R is the relative undeformed radius in the rolling direction ($1/R = 1/R_1 + 1/R_2$), P' is the load per unit axial contact width (or 2/3 of the width of elliptical or circular contacts), μ_o is the absolute viscosity at atmospheric pressure, γ is the pressure coefficient of viscosity in the formula $\mu = \mu_o e^{\gamma p}$ (where p is pressure), V is the total rolling velocity ($V = V_1 + V_2$), and E' is a reduced Young's modulus defined by the formula

$$\frac{1}{E'} = \frac{1 - \nu_1^2}{\pi E_1} + \frac{1 - \nu_2^2}{\pi E_2} \quad ,$$

where ν_1 and ν_2 are Poisson's ratios and E_1 and E_2 are Young's moduli for the rolling surfaces.

Some of the minimum-film-thickness data for the three lubricants in Table 1 are plotted versus load in Figure 8. Curves for the above two theoretical formulas, calculated for a 15-cs white oil at a rolling speed of 7000 fpm, are shown for comparison. Film-thickness data on the silicone, white oil, and diester lubricants reported previously[3,4] are also shown for comparison (these previous data are shown as the solid points in Figure 8). It can be seen from Figure 8 that the effect of load on the film thickness was usually greater than predicted by the elasto-hydrodynamic theories which assume an isothermal Newtonian lubricant. Increasing the rolling speed tended to increase the dependence of film thickness on load, as illustrated by the two curves for white mineral oil in Figure 8, at rolling speeds of 2600 and 7000 fpm. There was also a noticeable increase in the slope of the load-film thickness curves at high loads for some of the lubricants. In particular, this increase in load-film thickness slope became more pronounced with the engine oil at high temperatures even though the viscosity (29 cs) and the rolling speed (2600 fpm) were rather moderate. In general, however, the deviation of the experiments from the theories, in regard to the effect of load on film thickness, increased with increasing speed, load, and temperature level.

Minimum film-thickness data are plotted versus the bulk lubricant viscosity coefficients at the measured disk surface temperature in Figure 9. The product of the viscosity at atmospheric pressure and the pressure coefficient of viscosity was used since the physical properties of lubricants appear in the film-thickness theories essentially in terms of this product. The points in Figure 9 were limited to a narrow range of load equivalent to about 130,000 psi maximum contact pressure, or about 2500 pounds per inch of equivalent contact width. The fairly good fit of 38 experimental points to the smooth curves in Figure 9 for the white oil and polyphenyl ether at 7000 fpm rolling speed demonstrates the reproducibility of these data.

Theoretical curves for the two rolling speeds, 2600 and 7000 fpm, and a few previous experimental data at 2600 fpm speed are also shown for comparison. The agreement between the previous data and theory was good,

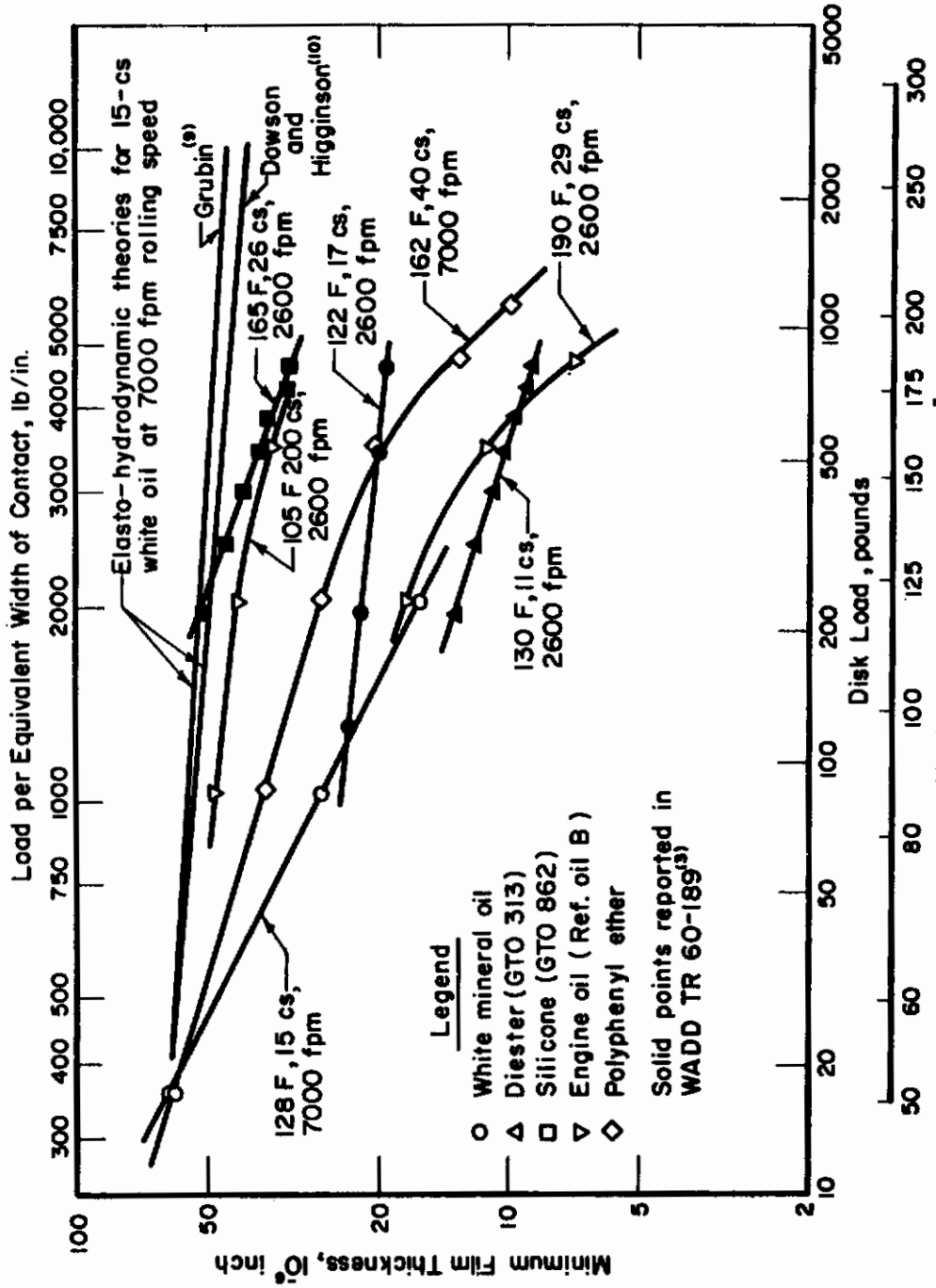

FIGURE 8. EFFECT OF LOAD ON FILM THICKNESS

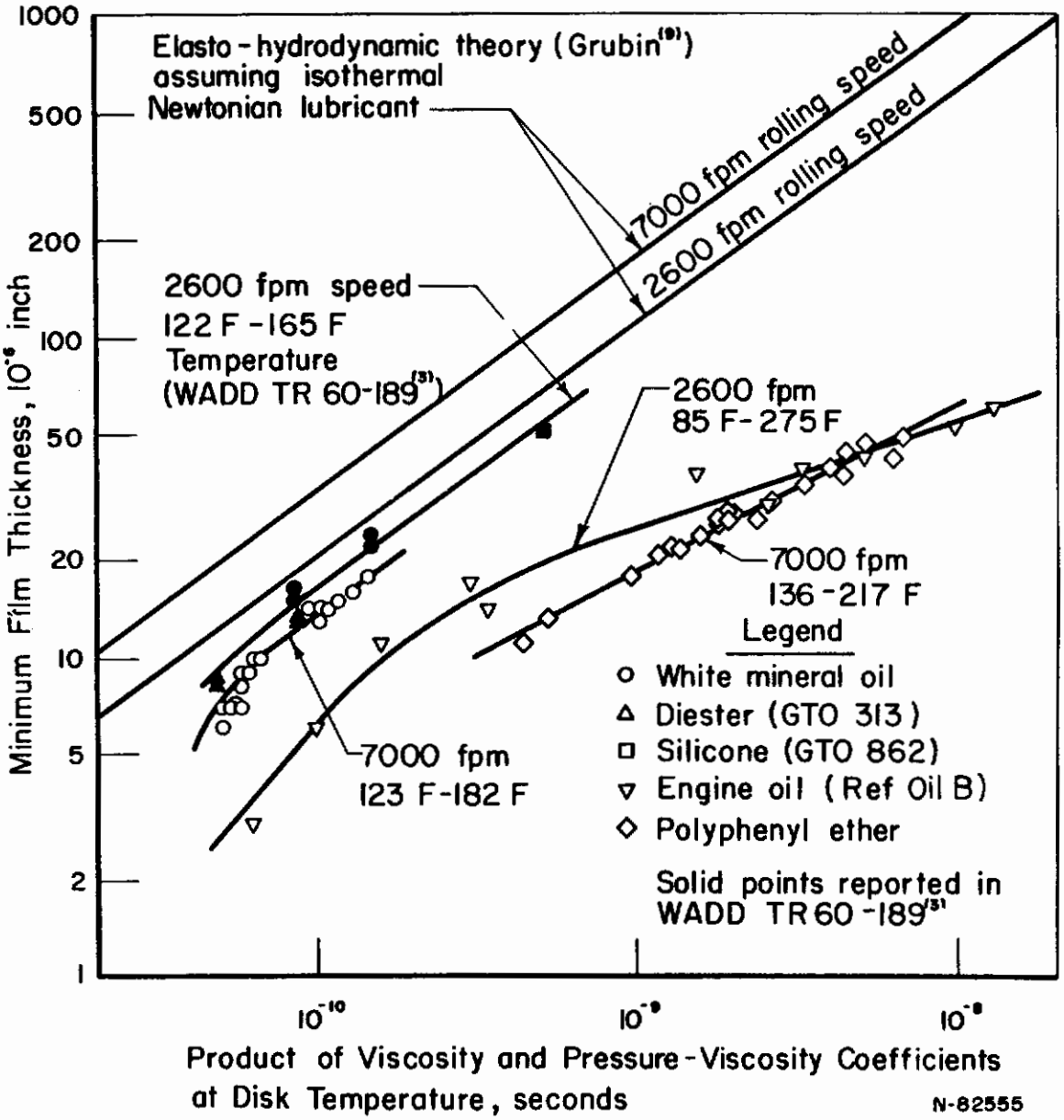

FIGURE 9. EFFECT OF AMBIENT TEMPERATURE AND VISCOSITY COEFFICIENTS ON FILM THICKNESS

Maximum load pressures 120,000 to 140,000 psi.

considering the effects of the slight compressibility of the lubricant and the deformed shape of the contact on the X-ray measurements of film thickness. The lubricant is probably compressed 15 to 20 per cent in the high-pressure contact region, and since the theories assume an incompressible lubricant, the theoretical curves should be adjusted downward by about this amount. Also, recent measurements of the shape of the deformed contact region in the rolling direction by Crook[11] indicate that the film thickness near the trailing edge of the contact was about 15 per cent lower than the film thickness at the center of the contact. This surface protuberance at concentrated contacts is predicted by theory[12-17], and it was demonstrated qualitatively in the experiments of Smith[18]. Since its curvature is greater than the curvature of the undeformed disk surfaces, the X-ray beam may partially penetrate this protuberance. In addition, the effect of surface roughness in the contact region may result in a minimum film thickness measured by the X-ray method that is slightly different from the film thickness derived by theory in which perfectly smooth surfaces are assumed. The surface finish of the disks ranged from 3 to 5 microinches, rms, as determined by a profilometer, for the experiments reported here.

Even with appropriate adjustments for the above-mentioned film-thickness effects, however, the new experimental data falls far below the theoretical predictions. The deviation from theory was most pronounced at high rolling speeds and with high-viscosity lubricants. It is also apparent from the curve for the engine oil in Figure 9 that, even at the same low speed and same viscosity coefficients for which data were obtained previously with the white mineral oil, the measured film thicknesses were about a factor of three lower than theoretical. The only apparent difference in these two sets of mineral oil experiments is that the engine oil was operated at about a 100 F higher disk temperature than was the white oil for the same viscosity.

A general plot of all the film-thickness data in Table 1 is shown in Figure 10, using the dimensionless parameters taken from elasto-hydrodynamic lubrication theory that assumes an isothermal Newtonian lubricant. The large scatter of the experimental points in Figure 10 suggests that these dimensionless parameters, and the theory on which they are based, do not include all of the variables affecting the film thickness. The scatter increased markedly for data taken over the extended ranges of operating conditions as compared with the previous data taken over limited ranges of speed, load, viscosity, and temperature, represented by the solid points in Figure 10. Theoretical curves representing two separate solutions of elasto-hydrodynamic theory assuming an isothermal Newtonian lubricant[9, 17] are plotted in Figure 10, illustrating the remarkable agreement between these quite different theories. Except for the few data taken under rather mild operating conditions, however, the experimental film thicknesses ranged considerably below these theoretical curves. Also plotted in Figure 10 are two isolated numerical solutions to the theory by Sternlicht, et al. [19], in which the energy equation for viscous heating of the lubricant

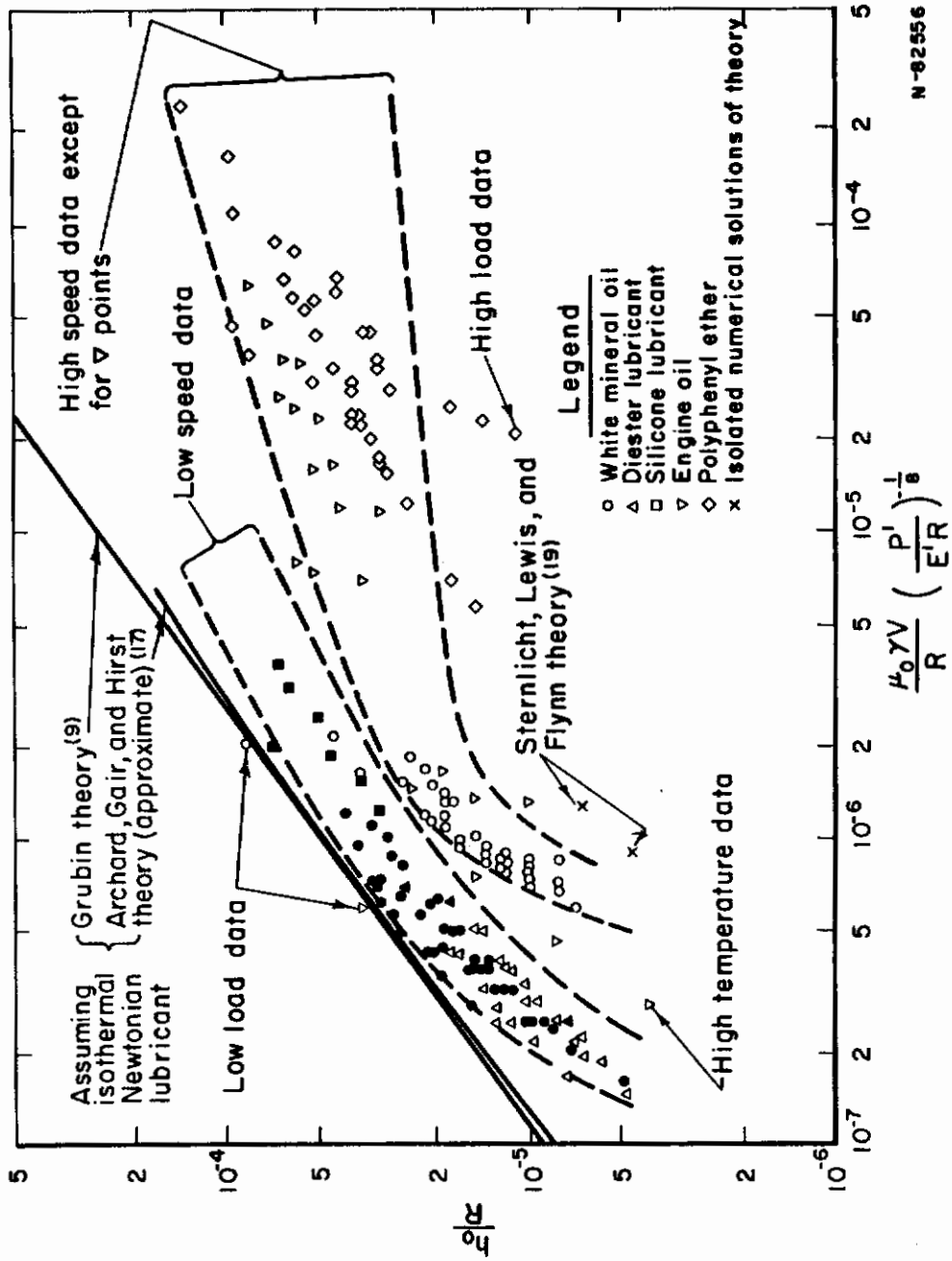

FIGURE 10. FILM-THICKNESS DATA COMPARED WITH ELASTO-HYDRODYNAMIC LUBRICATION THEORIES

was solved simultaneously with the elasto-hydrodynamic problem, assuming adiabatic conditions in the lubricant film. Although there are not yet enough solutions to this theory to demonstrate the generality of these isolated points, it does appear that the adiabatic assumption predicts film thicknesses that are too small.

Contact-Deformation Measurements

As described previously, the contour of the deformed contact region between the rolling disks can be plotted by moving the entire disk machine on ball-and-runner tracks across the narrow, stationary X-ray beam. In this way the distance between the surfaces, averaged around the circumference of the disks, is measured as a function of axial position. Since the two disk surfaces are finished in the same way by the same techniques, it is assumed that the contact-deformation profiles obtained in this manner represent twice the deformation on each disk. There is, of course, still some inherent error between the actual deformations and the recorded profiles, since an X-ray beam of finite width is used. However, this error was found by calculation to be slight for the present geometry of the system, and comparative measurements between profiles obtained under different operating conditions should still be realistic.

Another source of significant error in the contact-deformation measurements was the slight variation in the transverse curvature of the disks produced during successive relapping of the contacting surfaces. It was found that any slight variation in the lapping procedure, such as lap load or grit size, would produce a different transverse curvature, even though the lap is constructed to generate a constant 36-inch radius. The transverse radius of curvature was measured independently of the X-ray system using an electrolimit gage accurate to about 10 microinches. These data for the two disks used in the experiments reported here are plotted in Figure 11. It can be seen that the actual surface contours on these disks were very close to a true 36-inch radius of curvature in the regions where the deformation was measured during rolling contact.

Typical contact-deformation profiles under increasing load at constant lubricant viscosity and rolling speed (40-cs polyphenyl ether, 7000 fpm) are shown in Figure 12. At a 17-pound load (50,000 psi calculated maximum Hertz pressure), the rollers were essentially undeformed. Such conditions can presumably be described by ordinary hydrodynamic lubrication theory, including, of course, the increase in viscosity of the lubricant at these pressures. As the load was increased, the contact surfaces spread out elastically, indicating that elasto-hydrodynamic conditions prevailed. For comparison, three previous contact-deformation profiles are shown in Figure 12 for a 15-cs white mineral oil at 2600 fpm rolling speed, corresponding to loads equivalent to the three intermediate loads for the

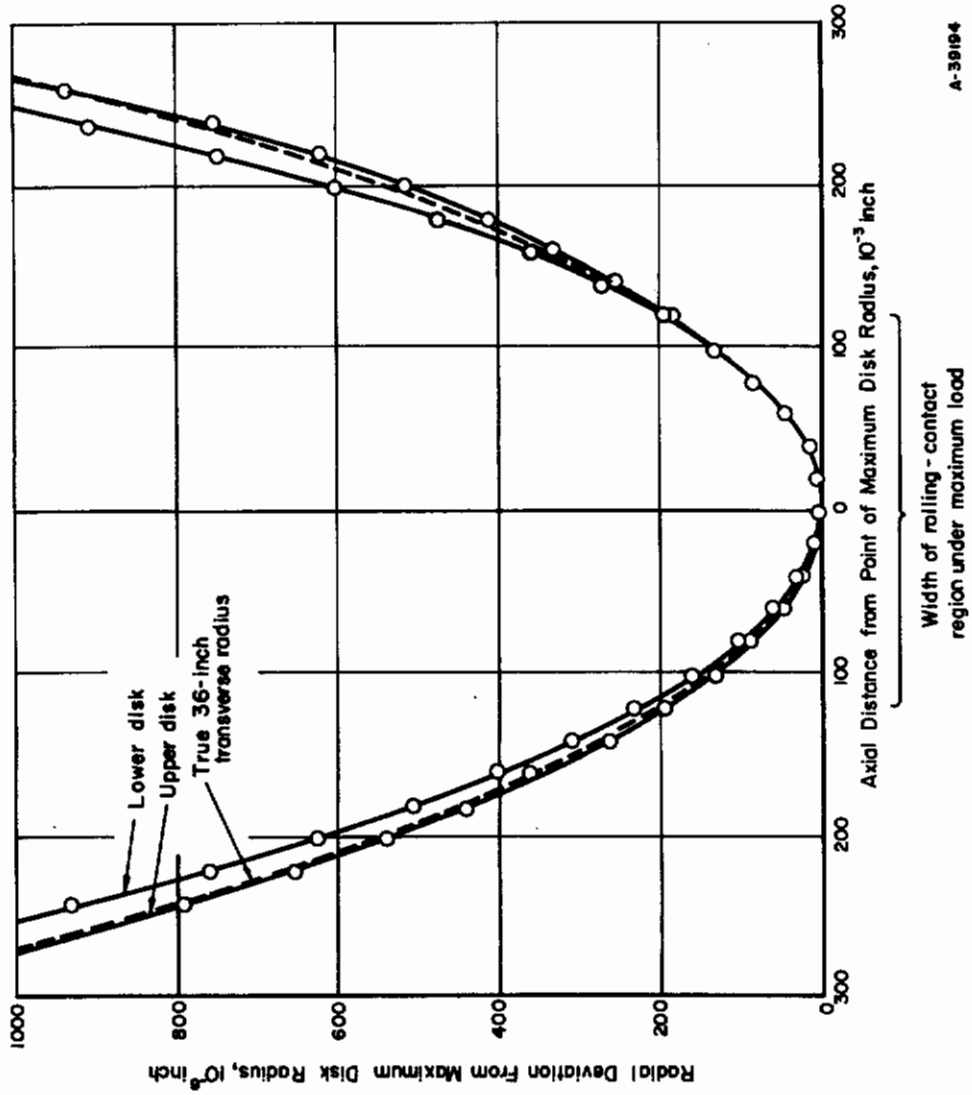

FIGURE 11. TRANSVERSE PROFILE MEASUREMENTS ON DISK SURFACES WITH ELECTROLIMIT COMPARATOR

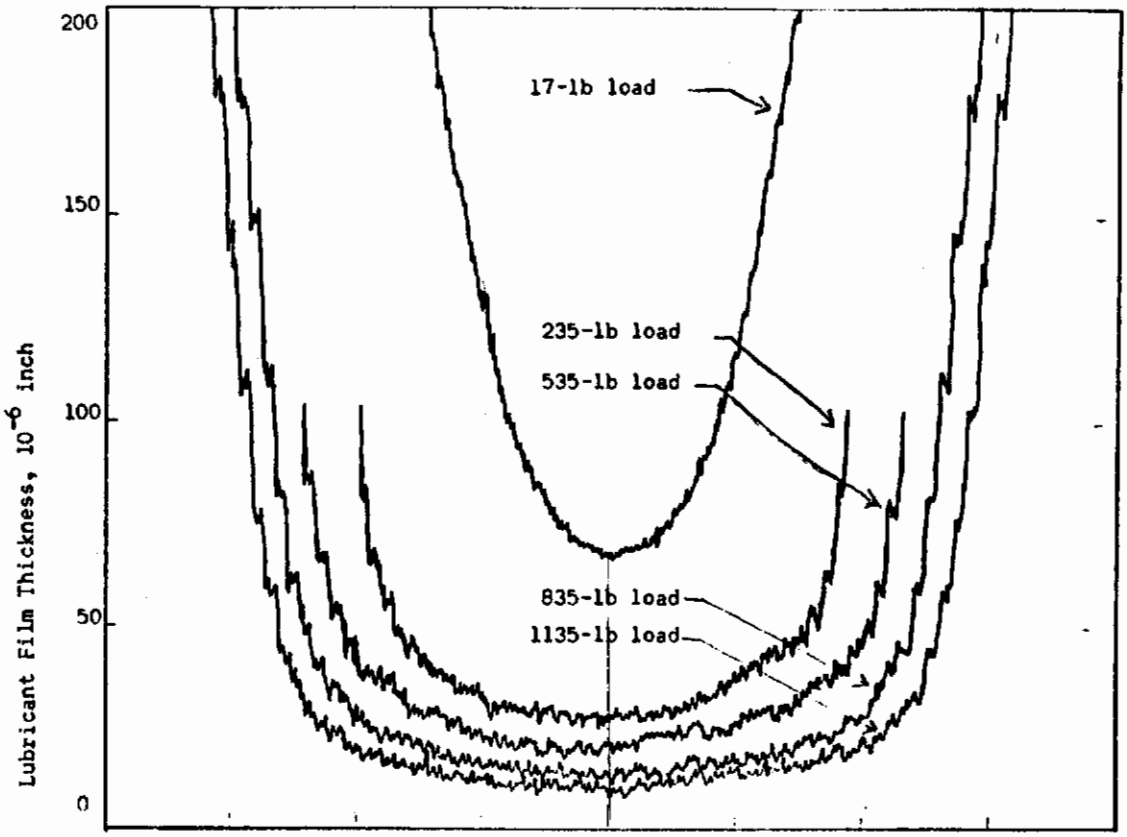

a. 40-CS Polyphenyl Ether (160 F) at 7000-FPM Rolling Speed

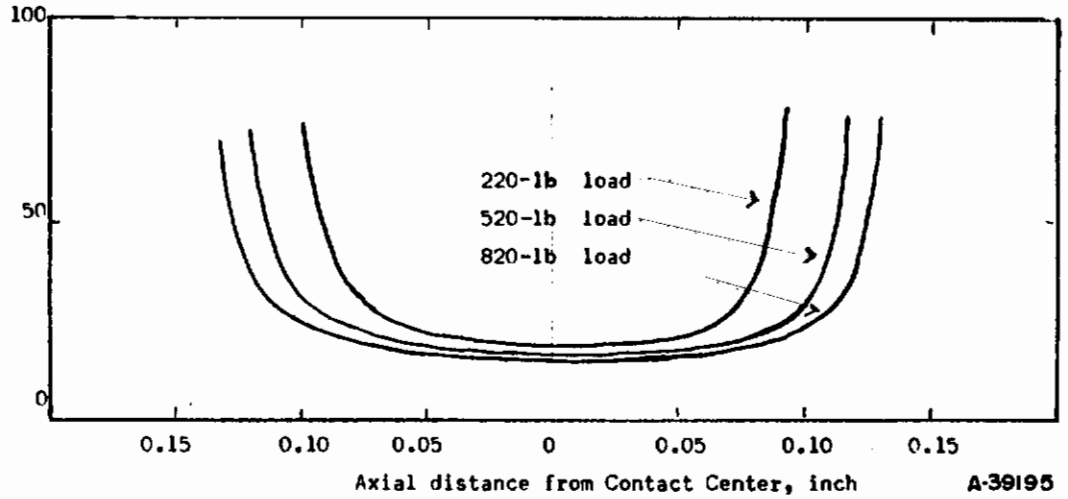

b. 15-CS White Mineral Oil (128 F) at 2600-FPM Rolling Speed

FIGURE 12. CONTACT DEFORMATION OVER A WIDE RANGE OF LOAD AT CONSTANT VISCOSITY AND SPEED

polyphenyl ether at high speed. These curves show that the effect of load on minimum film thickness for the white oil is smaller than that for the polyphenyl ether, as plotted before in Figure 8. In addition, they show that the white oil produced flatter contact regions with sharper corners at the edges of the contact than did the polyphenyl ether at the higher rolling speed.

The effect of speed and load on contact deformation with white mineral oil is shown in Figure 13, which presents data taken at rolling speeds corresponding to about 1.25×10^6 DN for 200-series ball bearings (DN is the bore diameter in millimeters times the shaft speed in revolutions per minute; 200-series bearings have a light cross section and are commonly used in aircraft). Two of the previously obtained low-speed profiles shown in Figure 12 are replotted in Figure 13 for a comparison of the deformation at equivalent loads. The increased effect of load on minimum film thickness and the increased rounding at the edges at the contact region at high rolling speeds is evident.

By far the most pronounced changes in film thickness and in the shape of the deformed contact surfaces, however, were caused by the viscosity of the lubricant. Some typical contact-deformation profiles in the direction transverse to the rolling direction are shown in Figure 14 for the engine oil at constant load and low speed (2600 fpm). Similar profiles for the cases when the disks are unloaded and when they are under static load are also shown to illustrate the effect of the lubricant. The profile under static load conforms closely to that which is predicted by Hertzian theory for dry static contact between curved elastic surfaces, suitably adjusted for the X-ray beam width and surface-roughness effects at the edges. The progressive rounding and narrowing of the contact region as the viscosity was increased is clearly shown in Figure 14. Similar effects of lubricant viscosity on contact deformation are shown in Figure 15 for the polyphenyl ether and in Figure 16 for the white oil, both at high rolling speed (7000 fpm).

Contact-deformation profiles for all three of these lubricants are compared at constant load and viscosity in Figure 17, in which smooth curves have been drawn through the recorder chart traces for easier comparison of the contact deformations. The profile for the white oil at 7000-fpm rolling speed, when compared with the curve taken from previous data for the same oil at lower speed (2600 fpm), illustrates the marked increase in the rounding of the contact with little change in minimum film thickness. (The diester lubricant used previously also produced contact deformations very similar to those for the white oil at low rolling speeds.) It should be noted that, at the particular load and viscosity plotted in Figure 17 (235 pounds and 12 cs), the two curves of minimum film thickness versus load for both the high and low speed, as plotted in Figure 8, are probably quite near their point of intersection. Since these curves have different slopes, even for the same oil and viscosity, the oil film is thinner at high speed for higher loads and thinner at low speed for lower loads than that for which Figure 17 is plotted.

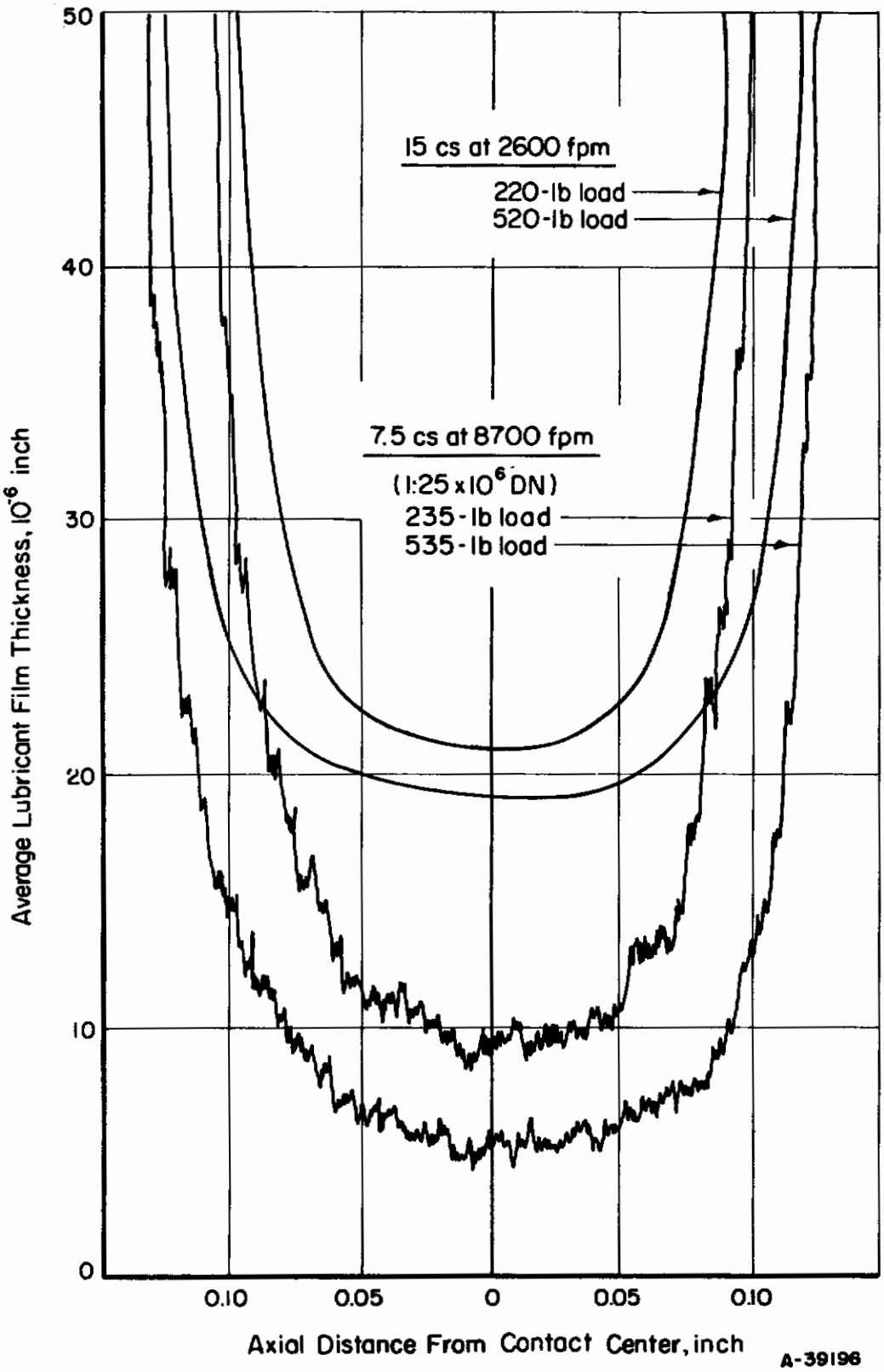

FIGURE 13. EFFECT OF LOAD AND HIGH ROLLING SPEED ON CONTACT DEFORMATION WITH WHITE MINERAL OIL

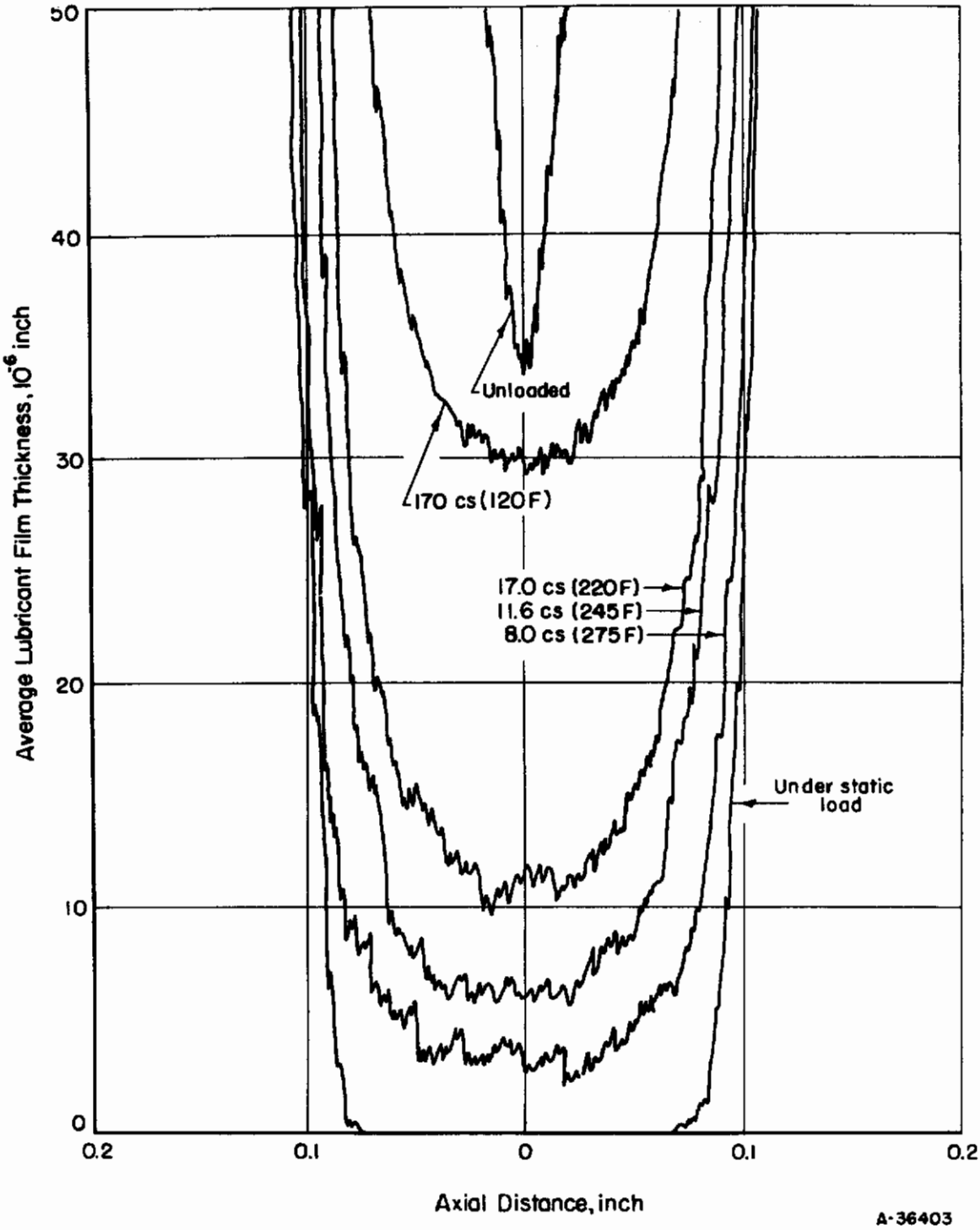

FIGURE 14. EFFECT OF VISCOSITY OF PETROLEUM OIL ON CONTACT DEFORMATION BETWEEN CROWNED ROLLERS

2600-fpm rolling speed, 385-lb load.

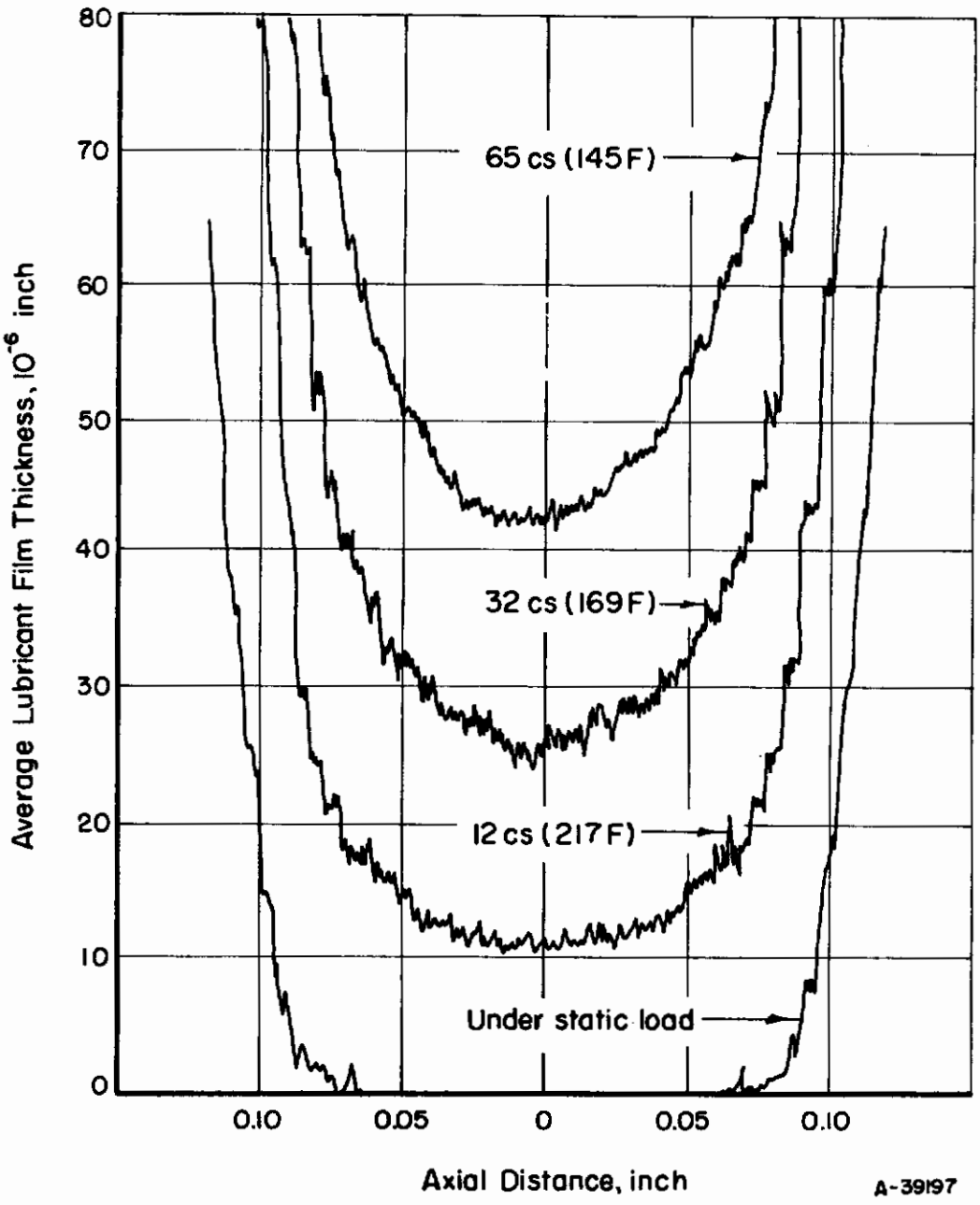

FIGURE 15. EFFECT OF VISCOSITY OF POLYPHENYL ETHER ON CONTACT DEFORMATION

7000-fpm rolling speed, 235-lb load.

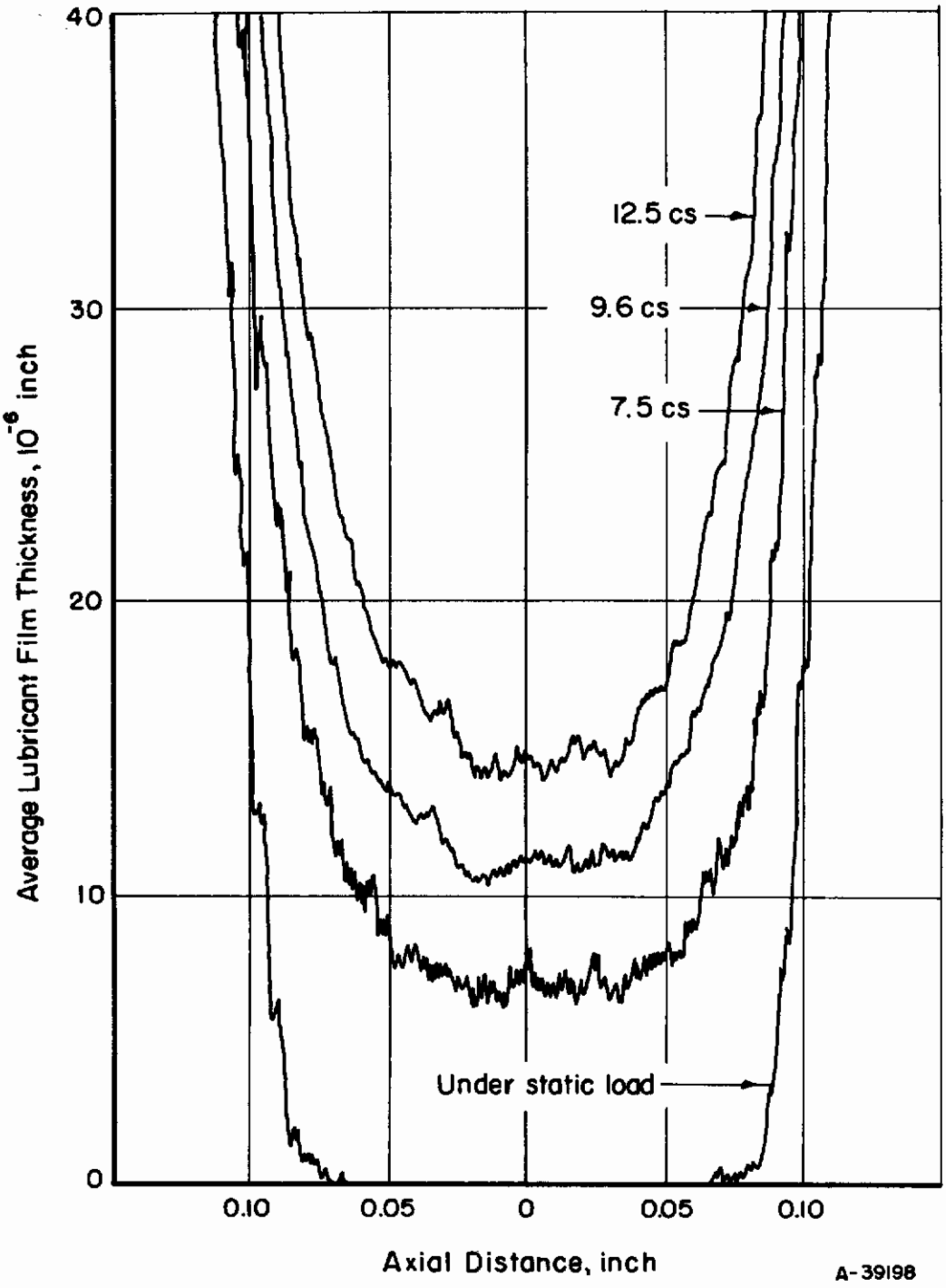

FIGURE 16. EFFECT OF VISCOSITY OF WHITE MINERAL OIL ON CONTACT DEFORMATION

7000-fpm rolling speed, 235-lb load.

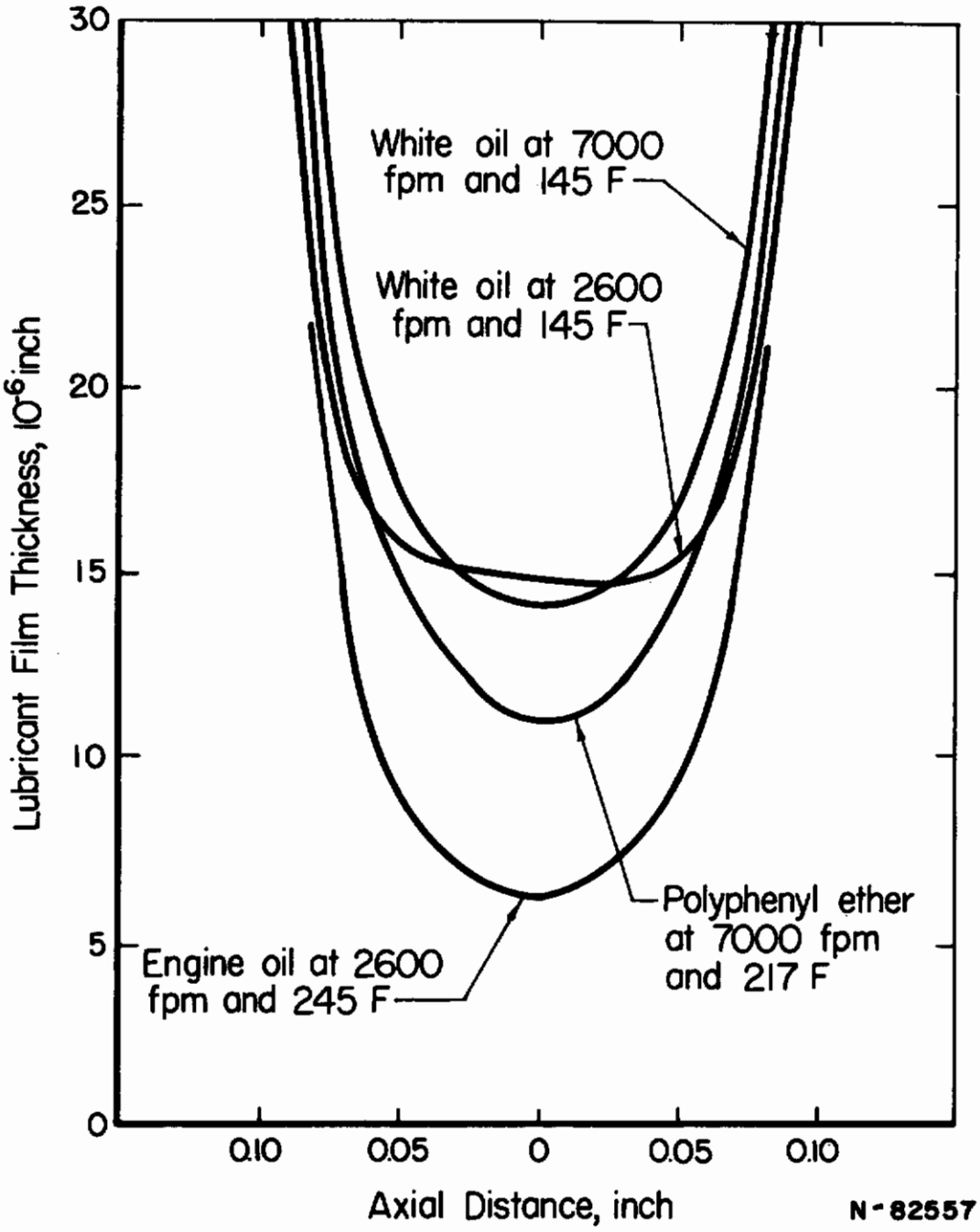

FIGURE 17. CONTACT DEFORMATION FOR DIFFERENT LUBRICANTS AND SPEEDS AT THE SAME LOAD (235 lb) AND VISCOSITY (12 cs)

The contact deformation with the polyphenyl ether, shown also in Figure 17, indicates a somewhat thinner film and perhaps somewhat more rounded or "pointed" shape than the profile for the white oil at the same viscosity and high-speed operating conditions. The increased rounding of the contact region and the thinner film with the engine oil than with the white oil or diester under the same low-speed operating conditions are even more pronounced. It would seem that the same effect that causes the thinner film may also cause a more rounded contact shape with both the engine oil and the polyphenyl ether than with the white oil or diester.

The changes in contact-deformation profile shown in Figures 12 through 17 reflect the changes in both the contact stresses in the rolling surfaces and the flow of the lubricant in the contact region. As the contact region became more rounded, the deformation deviated from the static and approached that which represented the unloaded or unstressed condition. Thus, the contact stresses must have decreased with increases in viscosity and rolling speed and with certain changes in lubricant type. This trend in contact stress caused by the lubricant correlates with the known effects of lubricant type and viscosity on rolling-contact fatigue. [20] It also correlates in some respects with the trends in deformation predicted by elasto-hydrodynamic lubrication theories in which the surfaces are allowed to deform elastically under the lubricant pressures, such as in the recent theory by Dowson and Higginson[15,16] and by Archard, Gair, and Hirst[17]. No simple comparison between these theories and the contact-deformation data can be made, however, since the theories provide only numerical solutions for profiles in the rolling direction for specific cases with cylindrical rollers, while the present results show only profiles in the transverse direction for spheroidal rollers. Even so, it is doubtful that such theories, if sufficiently broad, would predict the drastic reductions of the measured minimum film thickness below those obtained in the theory for rolling cylinders shown in Figures 8, 9, and 10. In fact, Archard and Kirk[6] show that the film thickness at point contacts between crossed cylinders, even with considerable sliding, is still about the same magnitude as in the rolling-disk machine operating under moderate conditions. Therefore, some characteristic of the lubricant not accounted for in the existing theories may cause the marked rounding of the contact surfaces and thinner minimum film thicknesses than predicted by theory at high loads, speeds, and viscosity and with certain lubricant types.

Several auxiliary studies were conducted during the course of these experiments with the engine oil (Reference Oil B). The lubricant is supplied to the contacting surfaces of the disks by a small jet (0.030-inch diameter) directed at the upper disk. The effect of lubricant flow rate was investigated by recording successive contact-deformation profiles as the flow rate was reduced. No significant change in the film thickness or the shape of the deformed surfaces was detected over a wide range of flow rates. Only after the lubricant was shut off did the film thickness decrease slowly. After about 4 minutes of running with no lubricant supplied to the disk surfaces (with the surface temperature remaining essentially constant at 115 F, corresponding to a lubricant viscosity of 150 centistokes), there seemed to be

significant breakdown of the lubricant film and some damage occurred to the disk surfaces. The surface temperature then increased during subsequent running, even after the supply of oil was restored. The above behavior is reminiscent of the behavior of engine mainshaft ball bearings operating under simulated engine conditions. (21) When the lubricant to such bearings was interrupted, an almost immediate increase in bearing noise was detected (with a much less viscous lubricant than that used in the disk machine), followed in a few minutes by thermal instability and bearing failure from loss of internal clearance. Examination of these bearing surfaces from interrupted-lubricant experiments which were stopped before failure revealed some superficial roughening of the surfaces. Behavior in the disk apparatus under these conditions, therefore, is similar to actual turbine ball-bearing performance.

An interesting phenomenon occurred in connection with the inadvertent scuffing of the disk surfaces caused by oil starvation of the contact region during the experiments on the effect of lubricant-flow interruption. Under high load the contact-deformation profiles indicated a definite ridge or asperity in the contact region extending an average of 15 microinches above the mean surface curvature, as shown in the first profile in Figure 18. This ridge all but disappeared when the load was reduced from 835 to 85 lb, shown in the second profile. When the load was increased again to 835 lb, the ridge increased to approximately its original size. The effect of surface roughness, or scuffing, on rolling-contact lubrication is a complicated, although important, aspect of lubricant behavior. A possible explanation of these results is that local heating in the lubricant film at points of reduced film thickness on surface asperities could have caused local thermal expansion of these asperities. If this effect has thermal causes, then the cyclic thermal stresses imposed on surfaces that exceed a certain critical roughness may contribute significantly to fatigue or other surface failure.

Development of Elasto-Hydrodynamic Theory For a Non-Newtonian Lubricant

The X-ray film-thickness measurements in the disk machine have shown differences in minimum film thickness and contact-deformation profile with different lubricants, even when they have essentially the same coefficients of Newtonian viscosity and pressure-viscosity. As will be discussed later, it is not likely that temperature variations in the film or variations in the experiments can explain all of these anomalous results. Therefore, it is desirable to examine how certain non-Newtonian characteristics of lubricants might affect rolling-contact lubrication. Specifically, a broader solution to the problem would be obtained if Grubin's theory for lubricant film thickness (9) could be modified to allow non-Newtonian behavior of the lubricant. The particular model for the lubricant to be examined here is the Ree-Eyring (22), as promoted by Hahn (23).

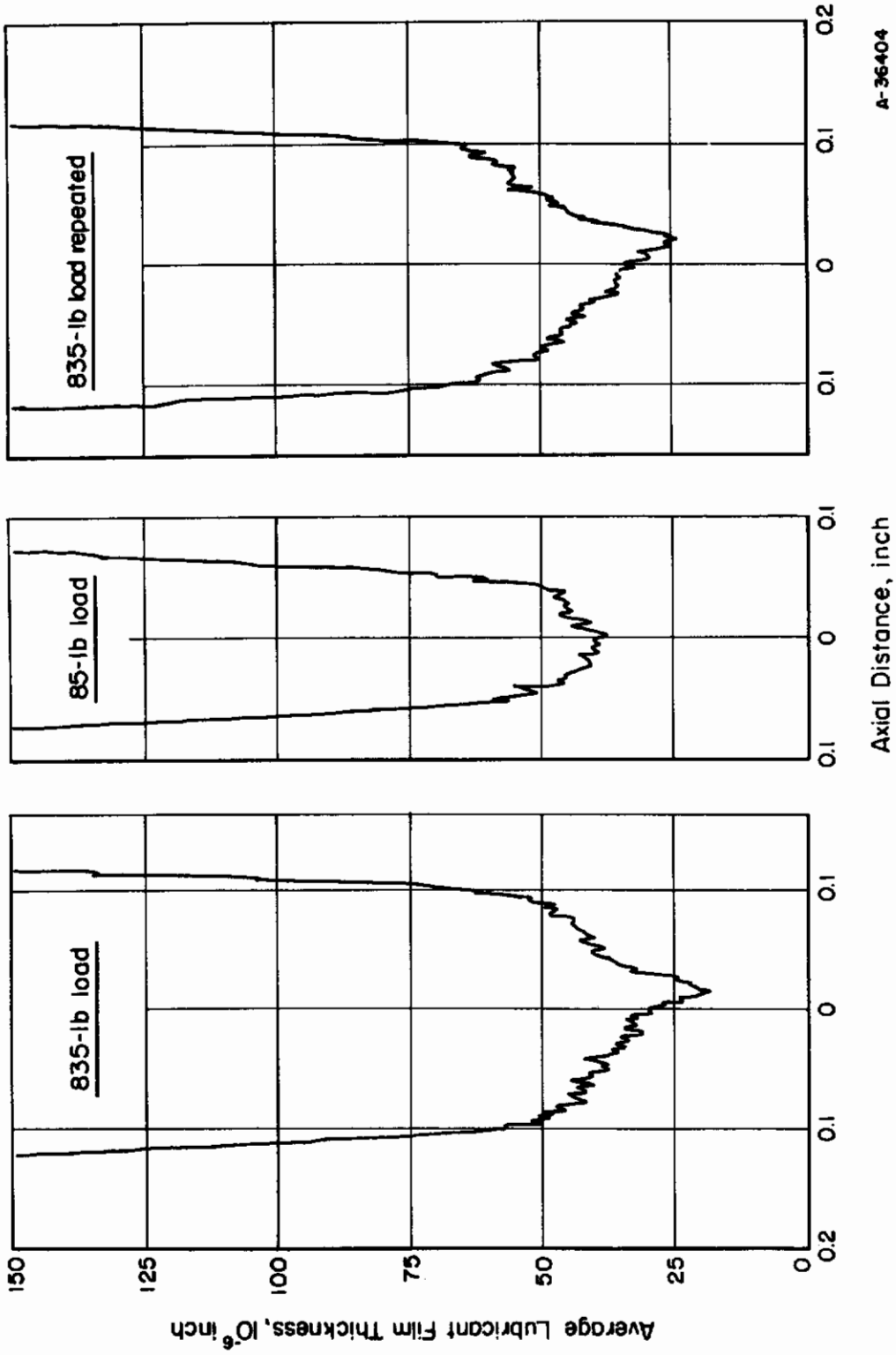

FIGURE 18. SEQUENCE OF CONTACT-DEFORMATION PROFILES SHOWING AN ASPERITY RIDGE (PERHAPS THERMALLY INDUCED) AT HIGH LOAD ON ROUGHENED SURFACES

2600-fpm rolling speed, 135 F Reference Oil B lubricant (110 cs).

In Reference (3), a lubricant-flow equation based on the Ree-Eyring model was developed. If, in addition to this equation, it is assumed (as in Grubin's work) that the slit between the rollers is shaped as in dry contact, plus assuming a uniform translation of the rollers apart from each other, then only exit and entrance conditions need be added to define the film-thickness problem. Thus, a single, first-order but highly nonlinear differential equation for the unknown pressure distribution can be obtained. In addition, methods were developed for obtaining an approximate solution to this equation for the case of rolling contact by which the lubricant film thickness can be predicted for a non-Newtonian lubricant. (24) The results of this theory in comparison with the Grubin theory for a Newtonian lubricant are presented in Figure 19.

It can be seen that the dimensionless coordinates of Figure 19 are similar to those of Figure 10, on which the disk-machine film-thickness data are plotted, except that a new non-Newtonian dimensionless parameter, $4R/\beta_o V$, has been added to both coordinates. In addition, the non-Newtonian solution is presented as a family of curves in another non-Newtonian parameter, the ratio γ_2/γ_1. These new parameters are explained as follows.

Saying that a lubricant is Newtonian is equivalent to saying that the relation between shear stress τ and shear rate $\dot{s}$ in the lubricant has the form

$$\tau = \mu \dot{s} \quad ;$$

where μ is the coefficient of viscosity. As mentioned previously, the viscosity in elasto-hydrodynamic lubrication is usually taken to be

$$\mu = \mu_o e^{\gamma p} \quad ,$$

where μ_o is the viscosity at ambient pressure and temperature, p is pressure, and γ is the pressure coefficient of viscosity at the same ambient temperature.

In the Ree-Eyring model for a lubricant, however, the relation between shear stress and shear rate has the form

$$\tau = \frac{X}{\alpha} \sinh^{-1} (\beta \dot{s}) \quad .$$

Pressure enters the formula twice, since $X = X_o e^{\gamma_1 p}$ and $\beta = \beta_o e^{\gamma_2 p}$. For a particular lubricant at a constant temperature, the quantities α, X_o, β_o, γ_1, and γ_2 are constants. * The new quantity β is proportional to the relaxation time of the lubricant, and probably has about the same magnitude.

*In the notation of Hahn, et al., (23) these five quantities are α_2, K_o, β_{20}, $-\Delta V/RT$, and $\Delta V^{\pm}/RT$, respectively. Here T is the absolute temperature and R is the standard thermodynamic conversion factor (gas constant). These quantities are discussed by Hahn, et al. All of them depend on the temperature, except perhaps α_2 (22).

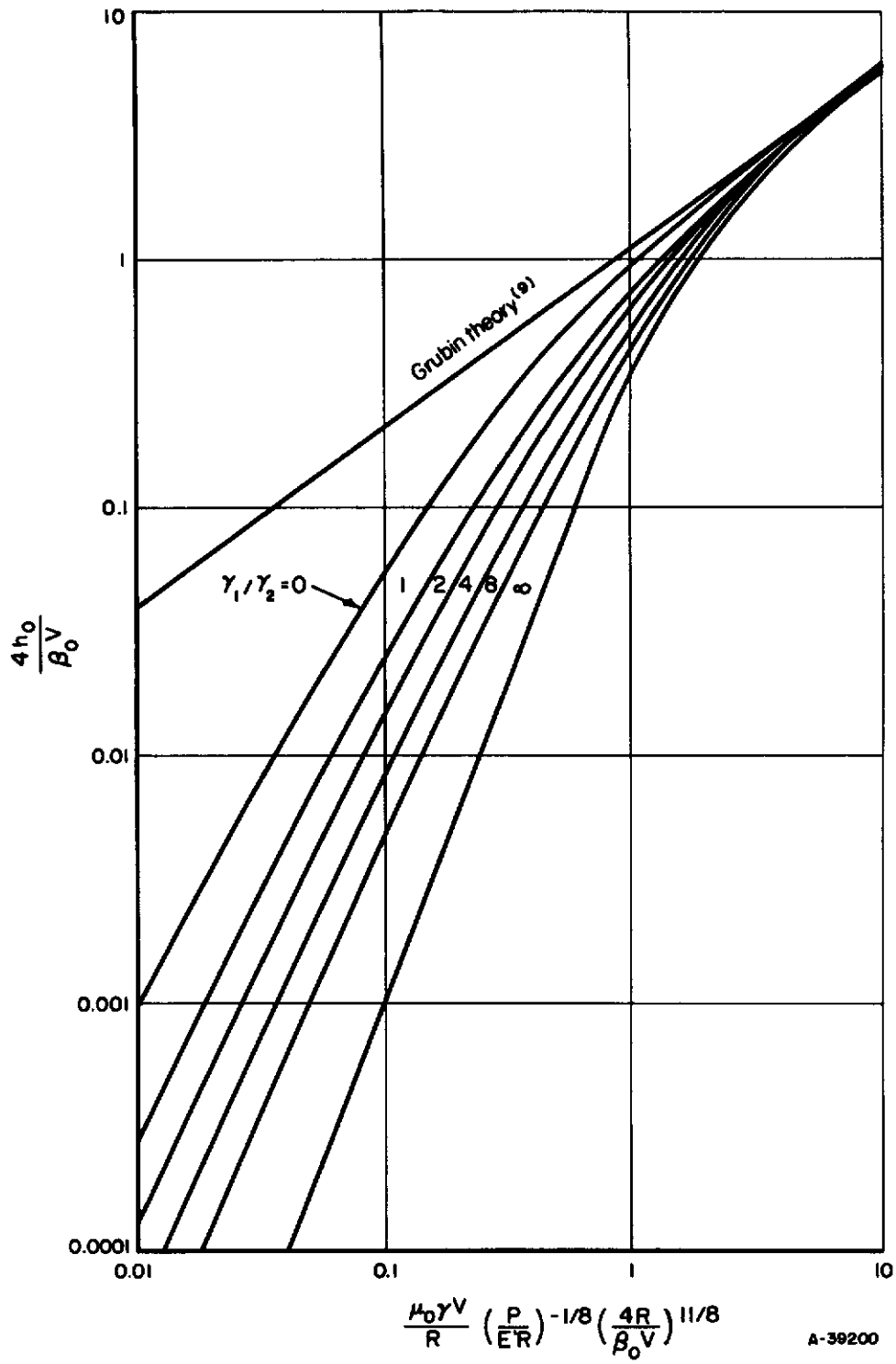

FIGURE 19. GRAPH FOR FINDING THE FILM THICKNESS OF A REE-EYRING LUBRICANT BETWEEN ROLLING CYLINDERS[24]

It can be seen further that whenever $\beta\dot{s} \ll 1$, then $\sinh^{-1}(\beta\dot{s}) \approx \beta\dot{s}$ and the Ree-Eyring model degenerates to

$$\tau = \frac{X\beta}{\alpha}\dot{s} = \frac{X_o\beta_o}{\alpha} e^{(\gamma_1 + \gamma_2)p}\dot{s} \quad .$$

This is the same as the Newtonian law with $\mu_o = X_o\beta_o/\alpha$ and $\gamma = \gamma_1 + \gamma_2$. Thus, it can be seen that, at low shear rates, the Ree-Eyring lubricant behaves in a Newtonian manner, but as shear rate increases, this model permits shear stress to develop at a lessening rate, owing to the $\sinh^{-1}$ function. The degree to which the shear stress is reduced (and to which the lubricant is non-Newtonian) depends on the relaxation time β_o and the ratio of the non-Newtonian to the Newtonian coefficients of pressure viscosity γ_2/γ_1.

In Figure 19, it is shown that lubricants will have a film thickness at rolling contacts significantly smaller than predicted by Newtonian theory if the parameter

$$\frac{\beta_o V}{h_o} > 1 \quad .$$

Thus, for a typical rolling velocity (2600 fpm) and film thickness (10^{-5} inch) this deviation will be significant for lubricants having a relaxation time greater than about 10^{-8} second, which is of the same order of magnitude as many common bearing lubricants[25]. In the non-Newtonian regime, of course, the deviation from Newtonian theory is greater for lubricants having a higher ratio of non-Newtonian to Newtonian pressure coefficients of viscosity. In order to apply this theory to the film-thickness measurements, however, it is necessary to measure experimentally these non-Newtonian properties of lubricants.

Development of a High-Pressure Lubricant Rheology Device

The high pressure rheology device is a machine designed to measure the viscosity of lubricants under extreme conditions of pressure, shear stress, and shear rate comparable to conditions experienced in aircraft rolling-contact bearings. Consideration of the operating parameters suggests that the lubricant should behave in a non-Newtonian manner, i. e., shear stress will cease to be proportional to shear rate, and the lubricant will yield almost in a plastic manner under high-shear conditions. The following sketch illustrates this type of non-Newtonian behavior which is believed to exist in rolling-bearing lubrication, as discussed previously.

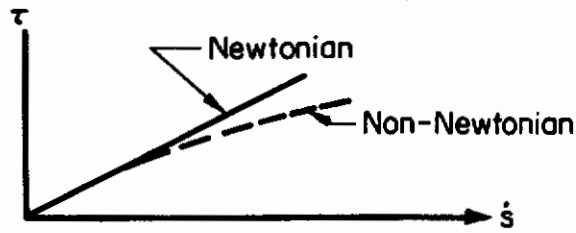

The knowledge of lubricant characteristics in this non-Newtonian regime is vital in understanding lubricant and bearing performance.

Description of Apparatus

The general concept of the high-pressure viscometer is illustrated in Figure 20. Air is supplied to the downstream piston, then oil is pumped into the central section, forcing the movable slug to the front of the central region and displacing the upstream piston outwards. The lubricant is now pressurized by means of a 30,000-psi capacity oil pump and by supplying a pressure to the upstream piston slightly less than the downstream pressure. The stroke consists of forcing an overpressure of air to the upstream piston and simultaneously bleeding the air back of the downstream piston; this is accomplished by means of an accumulator system, Figure 21. As the slug passes through the tube, an unbalanced pressure, proportional to the shear stress on the lubricant film between the slug and the tube, is developed across the slug. This unbalanced pressure creates a strain on the tube which is measured by a strain-gage system. The velocity, which is proportional to the shear rate, is measured by means of three position sensors stationed along the tube. Photographs of this high-pressure lubricant rheology machine and associated equipment are shown in Figures 22 and 23.

Although the basic concept of the rheology device is relatively straightforward, the actual design and development have presented some difficulties. The following is an enumeration of the more pertinent problems encountered.

The Bridgman unsupported area sealing principle was required for sealing the intensifier pistons against the high-pressure oil. Figure 24 is a sketch of the sealing mechanism developed commercially for use in the rheology device. Although this system is effective in sealing against the high pressure, as the pressure increases the sealing force increases causing a higher driving pressure required to actuate the viscometer.

The accumulator, Figure 21, is a device by which pressure is supplied to the upstream piston and simultaneously released from the downstream piston. The system uses constant-force spring motors which are intended to make this pressure constant during the stroke. The spring system,

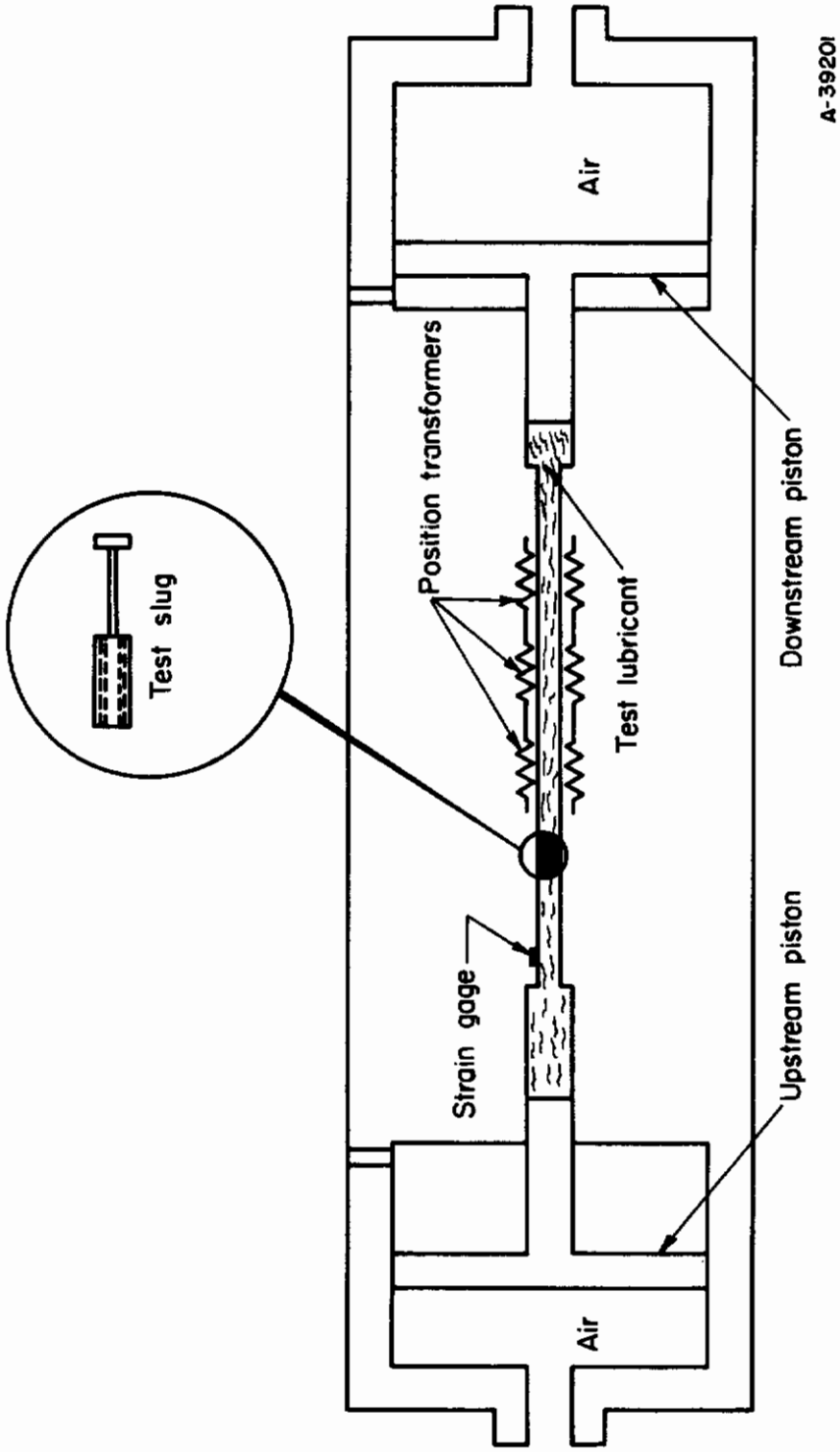

FIGURE 20. SCHEMATIC OF LUBRICANT RHEOLOGY DEVICE

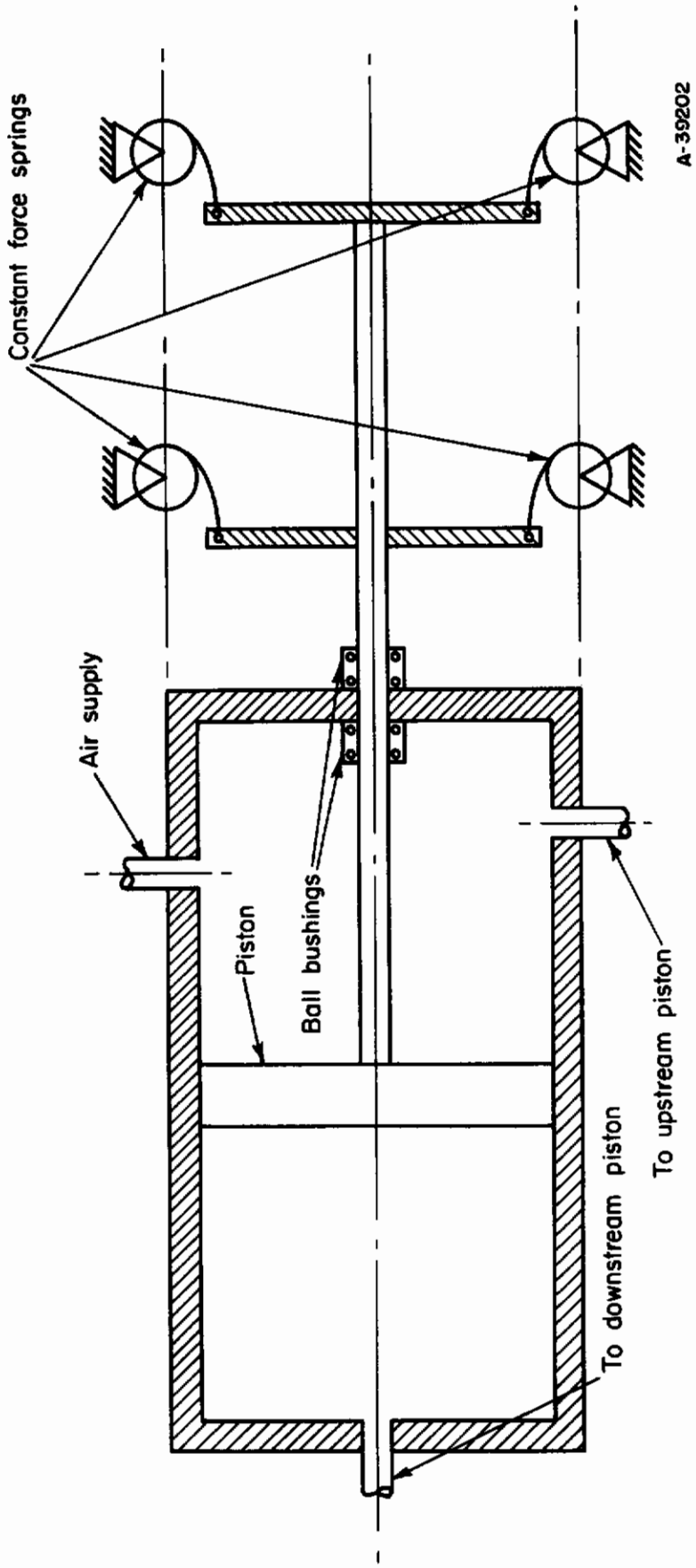

FIGURE 21. SCHEMATIC OF ACCUMULATOR SYSTEM

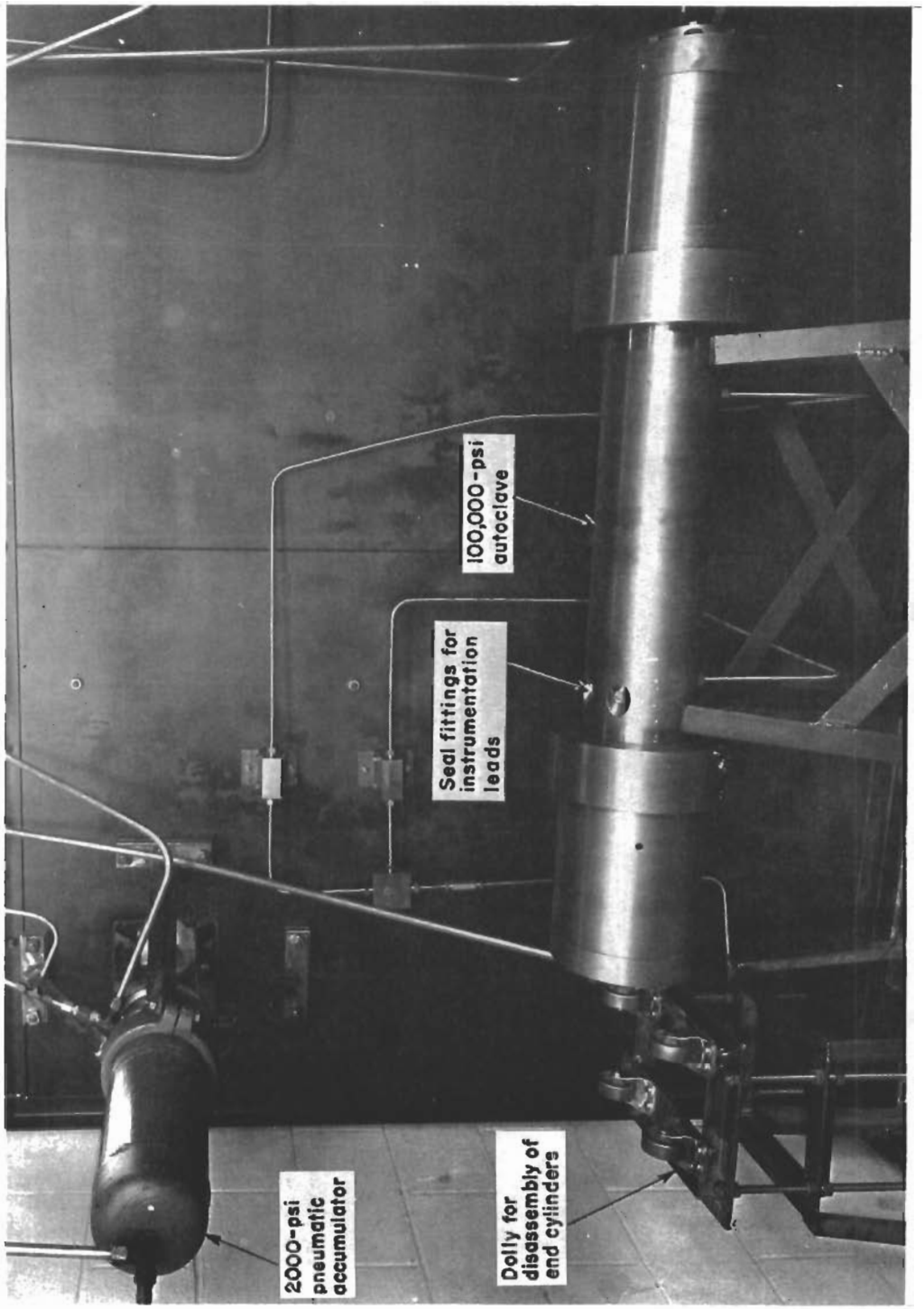

N72263

FIGURE 22. HIGH-PRESSURE LUBRICANT-RHEOLOGY RIG SHOWING PNEUMATIC ACCUMULATOR

N72262

FIGURE 23. CONTROL PANEL FOR HIGH-PRESSURE LUBRICANT-RHEOLOGY RIG

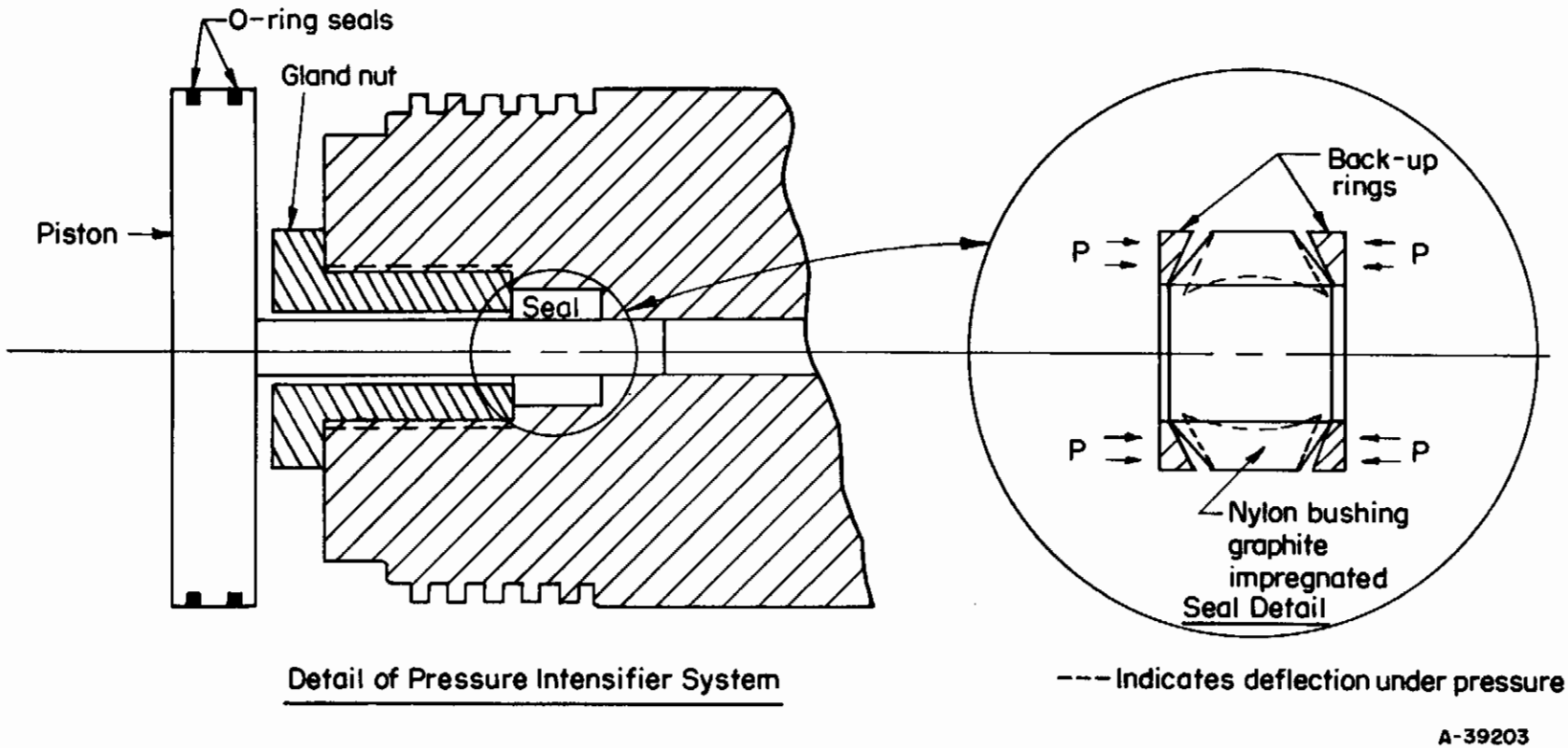

FIGURE 24. DETAIL OF INTENSIFIER PISTON-SEAL SYSTEM

however, has been found to exert an eccentric loading to the shaft which originally caused it to seize in its seal. This difficulty has been successfully eliminated by the addition of linear ball bushing supports.

Since no system for installing and sealing lead wires under extreme pressure could be found available commercially, it was necessary to develop such a system. The seal presently being used consists of leather and nylon packing threaded onto the lead wires and held by steel back-up rings (Figure 25). The wires selected to pass through this seal system had to be flexible, and be contained in an airtight insulation. Magnesium oxide insulated Chromel sheathed thermocouple wire has been found to be satisfactory in a static oil pressure up to 30,000 psi.

The velocity sensors are basically transformers with no core. A d-c current is supplied to the primary circuit; then, when the slug passes through the transformer, a voltage is induced into the secondary circuit (for instrumentation see Figure 26). Since the transformer wires are located directly on the tube, they had to be insensitive to oil pressure and small enough to fit in the available space. The transformers are made by bonding a sheet of Teflon over the tube, wrapping three coils of 100 wrappings each 0.5 inch wide and 2.5 inch apart, wrapping each coil with a small sheet of Teflon, and wrapping coils of 400 wrappings per coil on top of the original windings. Both the primary and secondary transformer circuits are wired in series with one end grounded to the tube and the other end attached to a lead wire.

An SR-4 Bakelite-backed strain gage proved to be unusable for strain measurements in the high-pressure oil. Experiments were conducted to determine a suitable method of measuring strain. Two types of strain gages were investigated, one was a weldable strain gage, the other was a ceramic stripable (no backing) gage. The ceramic gage gave reproducible readings, except for some relaxation effects in the 30,000-psi range, while the weldable gage appeared to be unsatisfactory.for the intended purpose. The experiment also indicated the necessity for two gages to balance out strain due to hydrostatic pressure. Even with two gages, one radial and one transverse, some drift was noticed in the readings as the static pressure was increased. Figure 27 presents this apparent strain versus hydrostatic-pressure buildup.

Preliminary Experiments and Discussion

Experiments have been performed on white mineral oil (105 SSU at 100 F) under hydrostatic pressures from 0 to 30,000 psi and using spring forces of from 300 to 1000 lb in the accumulator. On the basis of area ratios, the maximum overpressure available to the slug should be 3.26 times the spring force in psi. It appears that the majority of this pressure is lost in actuating the system because of seal friction. Some typical recorder traces are presented in Figures 28, 29, and 30. The chart speed was

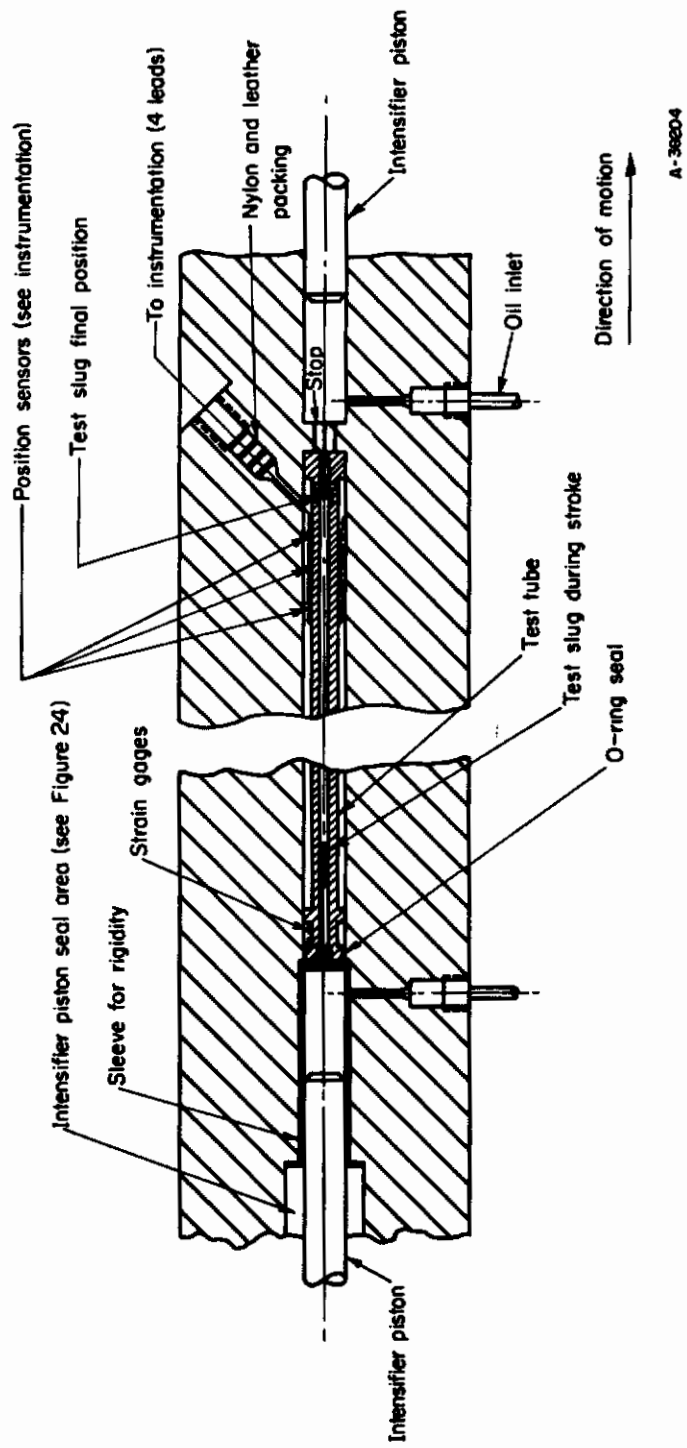

FIGURE 25. DETAIL OF TEST SECTION OF RHEOLOGY DEVICE

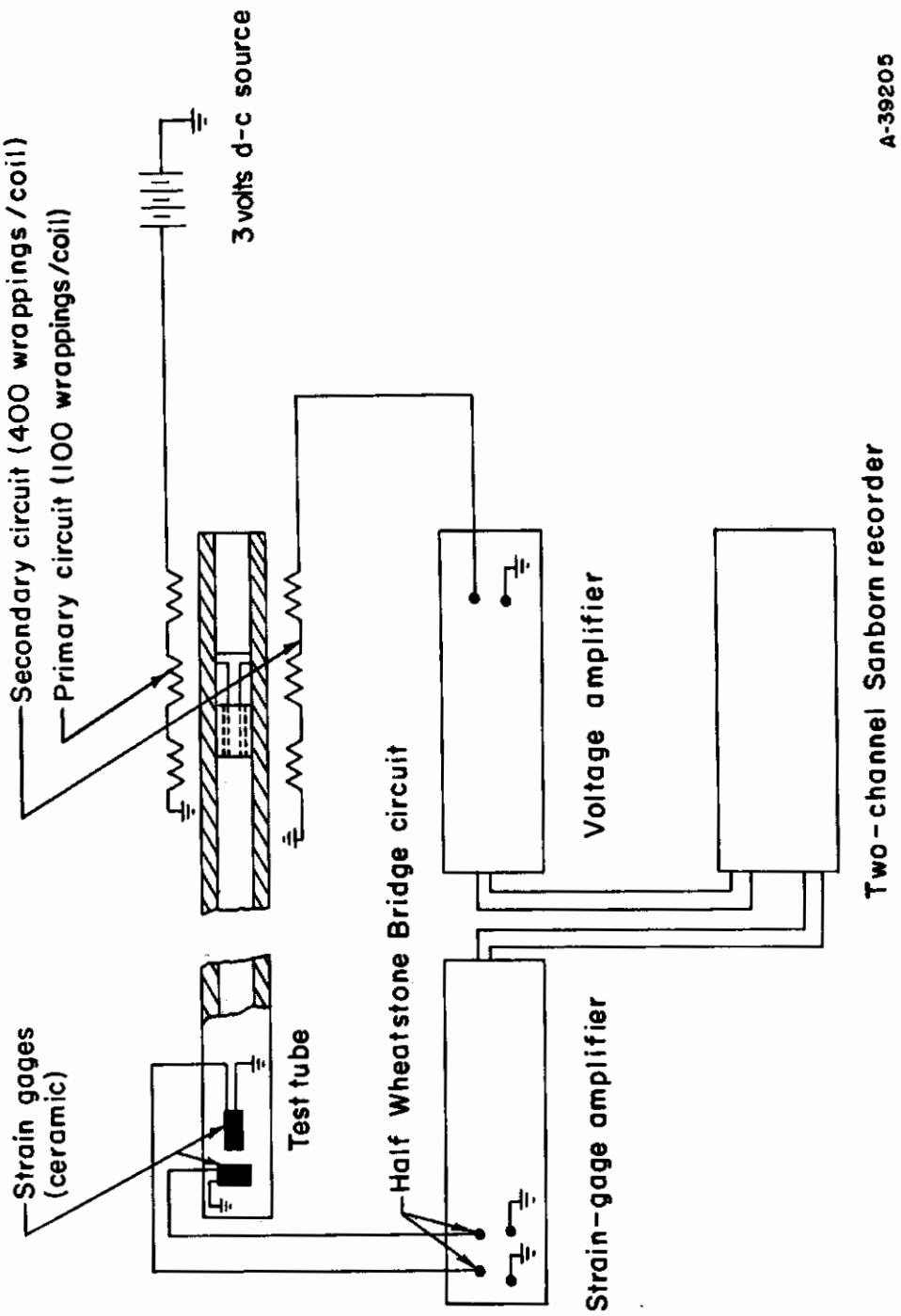

FIGURE 26. INSTRUMENTATION CIRCUIT DIAGRAM

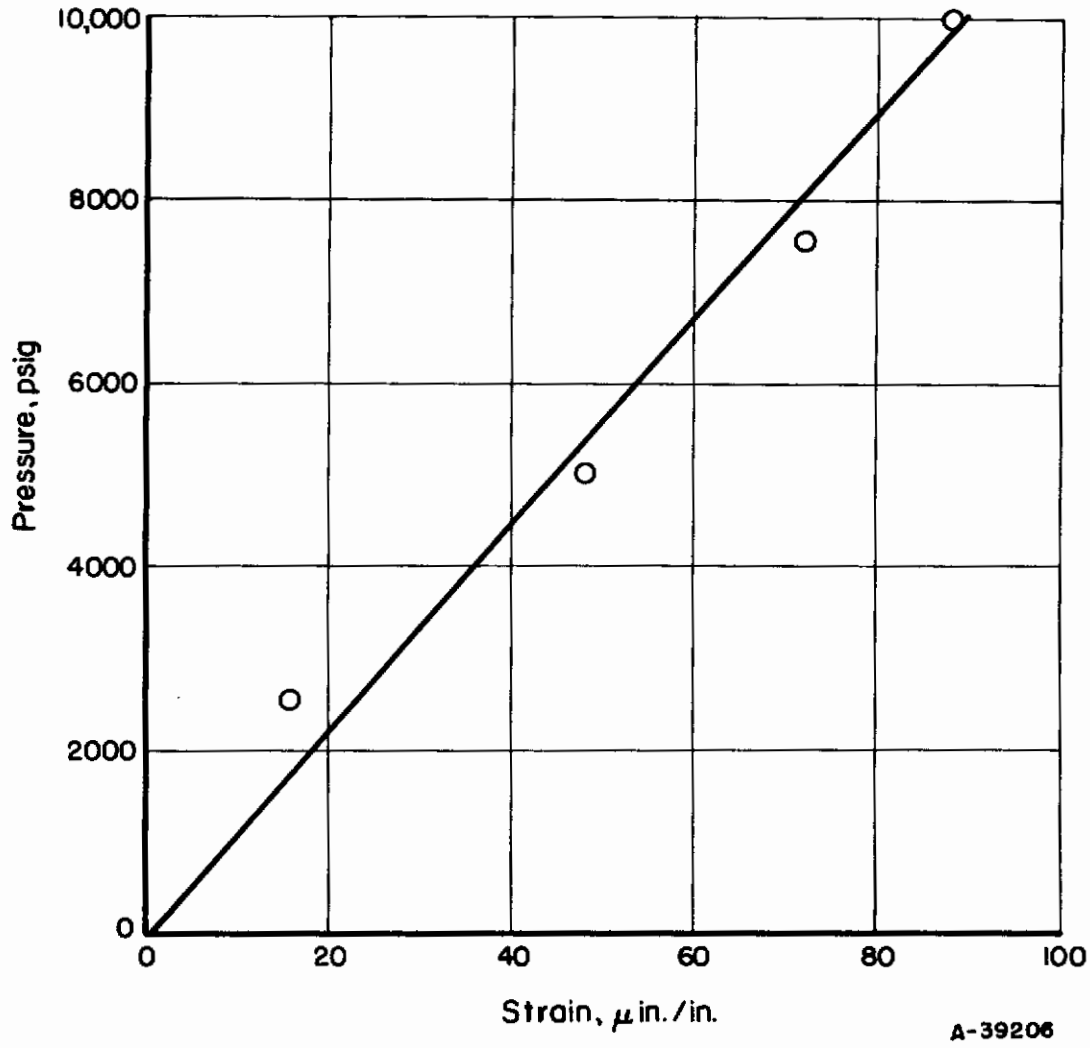

FIGURE 27. STRAIN GAGE DRIFT DUE TO STATIC PRESSURE BUILDUP

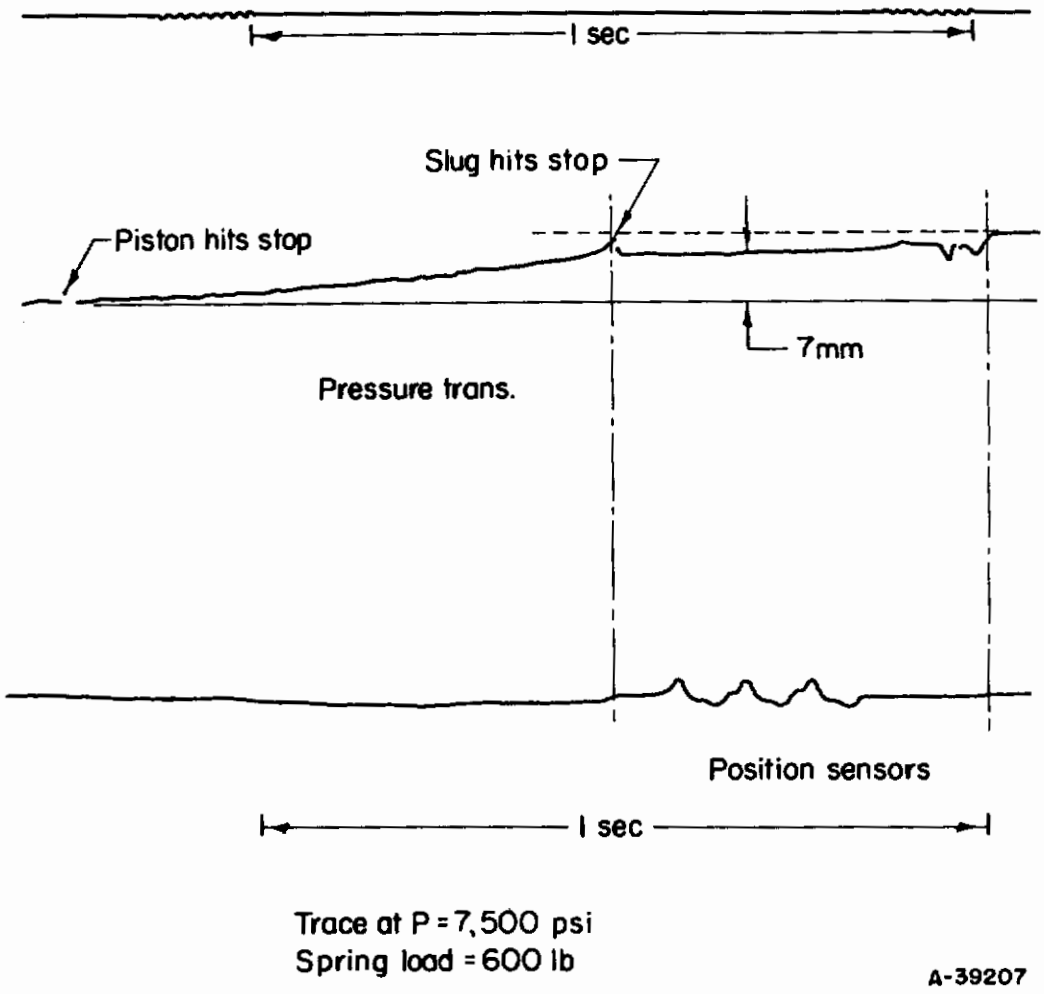

FIGURE 28. TYPICAL SANBORN TRACES SHOWING DRIVING PRESSURE AND SLIDER POSITION VERSUS TIME AT P_{static} = 7,500 psi

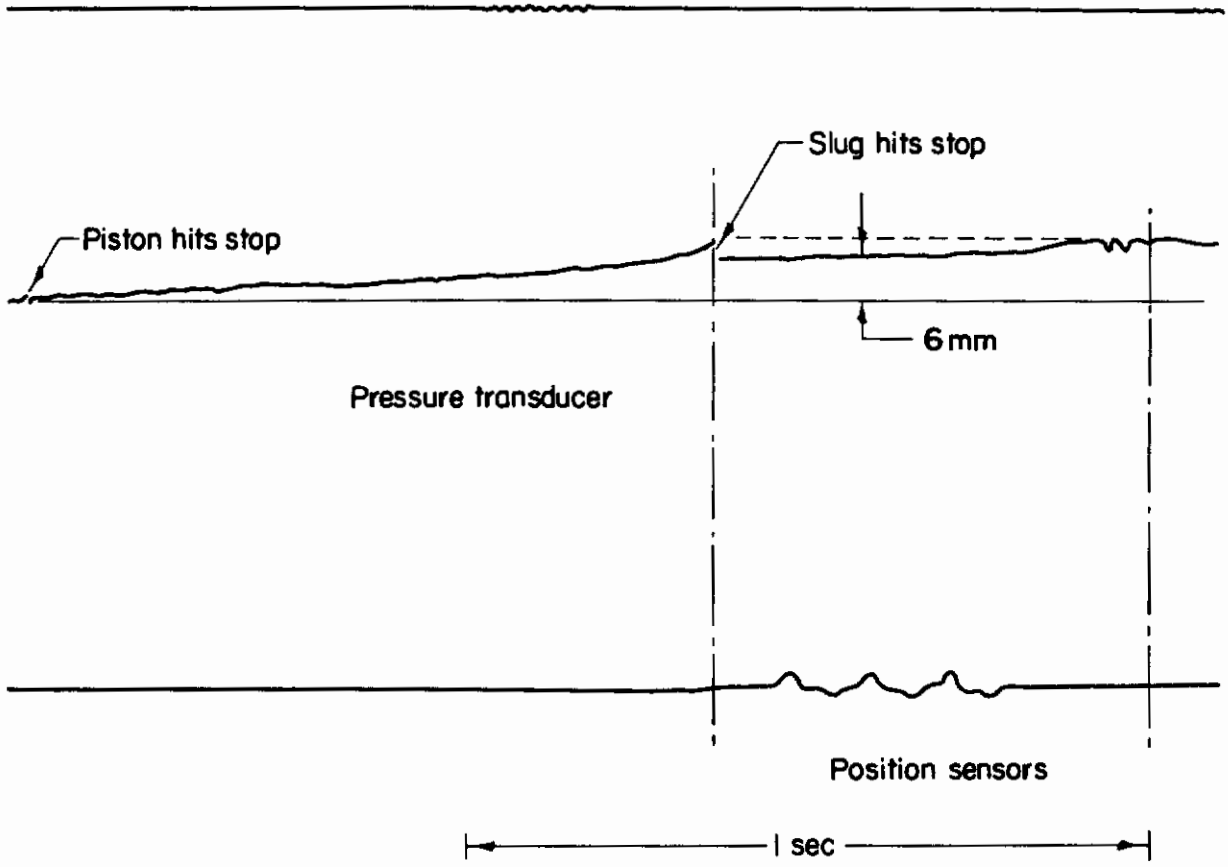

FIGURE 29. TYPICAL SANBORN TRACES SHOWING DRIVING PRESSURE AND SLIDER POSITION VERSUS TIME AT P_{static} = 10,000 psi

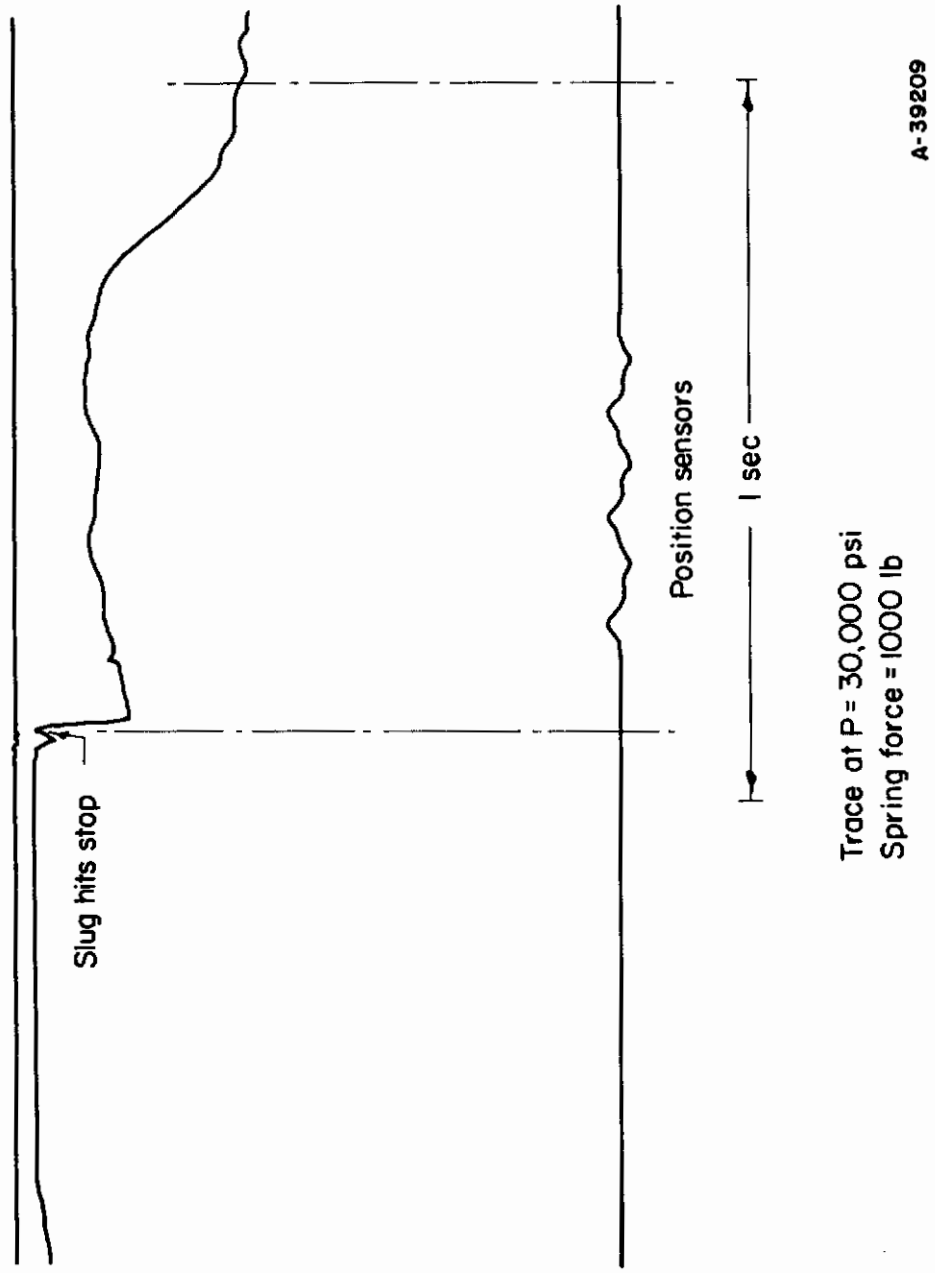

FIGURE 30. TYPICAL SANBORN TRACE SHOWING DRIVING PRESSURE AND SLIDER POSITION AT P_{static} = 30,000 psi

100 mm/sec and 1 mm deflection of the strain-gage trace represents 4 microinches of apparent strain. The calibration of the strain-gage circuit is shown in Figure 31.

Although the system is quite sensitive to small shear stresses, it is still difficult to interpret the data directly. A large hydrostatic pressure buildup is required to actuate the system. As was mentioned previously, this pressure buildup causes the strain gages to drift slightly. This drift is of the same order of magnitude as the strain due to shear stress. Therefore, a knowledge of the pressure during the stroke is pertinent in interpreting the results. Unfortunately, this pressure is not equivalent to the final pressure because the upstream piston bottoms first, allowing the pressure to relax while the downstream piston completes its stroke.

The following changes are being incorporated into the rig. A valve has been designed that will allow the pressure to stay constant for a short period following the stroke, thus allowing the dynamic pressure buildup to be read directly. An alternative system which can be used with the strain-gage system for measuring driving pressure by an external method has been designed, Figure 32. This device uses a flexible bellows and a differential transformer. The transformer will be mounted externally. This has the possible problem of excessive flow volume during a stroke and subsequently a time lag in reaching maximum deflections. However, basic calculations indicate that this time lag will be small and can be held to a minimum by means of a suitable spring.

DISCUSSION AND CONCLUSIONS

Lubricant-Film Thickness at Rolling Contacts

The minimum lubricant-film thickness between rolling disks, as measured by the X-ray method, was found to conform to the following formula under moderate operating conditions[3,4]:

$$\frac{h_o}{R} = 0.057 \left(\frac{P'}{E'R}\right)^{-0.36} \left(\frac{\mu_o \gamma V}{R}\right)^{0.73}$$

For point contacts between crossed cylinders operating under similar moderate conditions of speed, load, and lubricant viscosity, Archard and Kirk[6] found the following empirical formula for film thickness:

$$\frac{h_o}{R} = 0.028 \left(\frac{P'}{E'R}\right)^{-0.13} \left(\frac{\mu_o \gamma V}{R}\right)^{0.56}$$

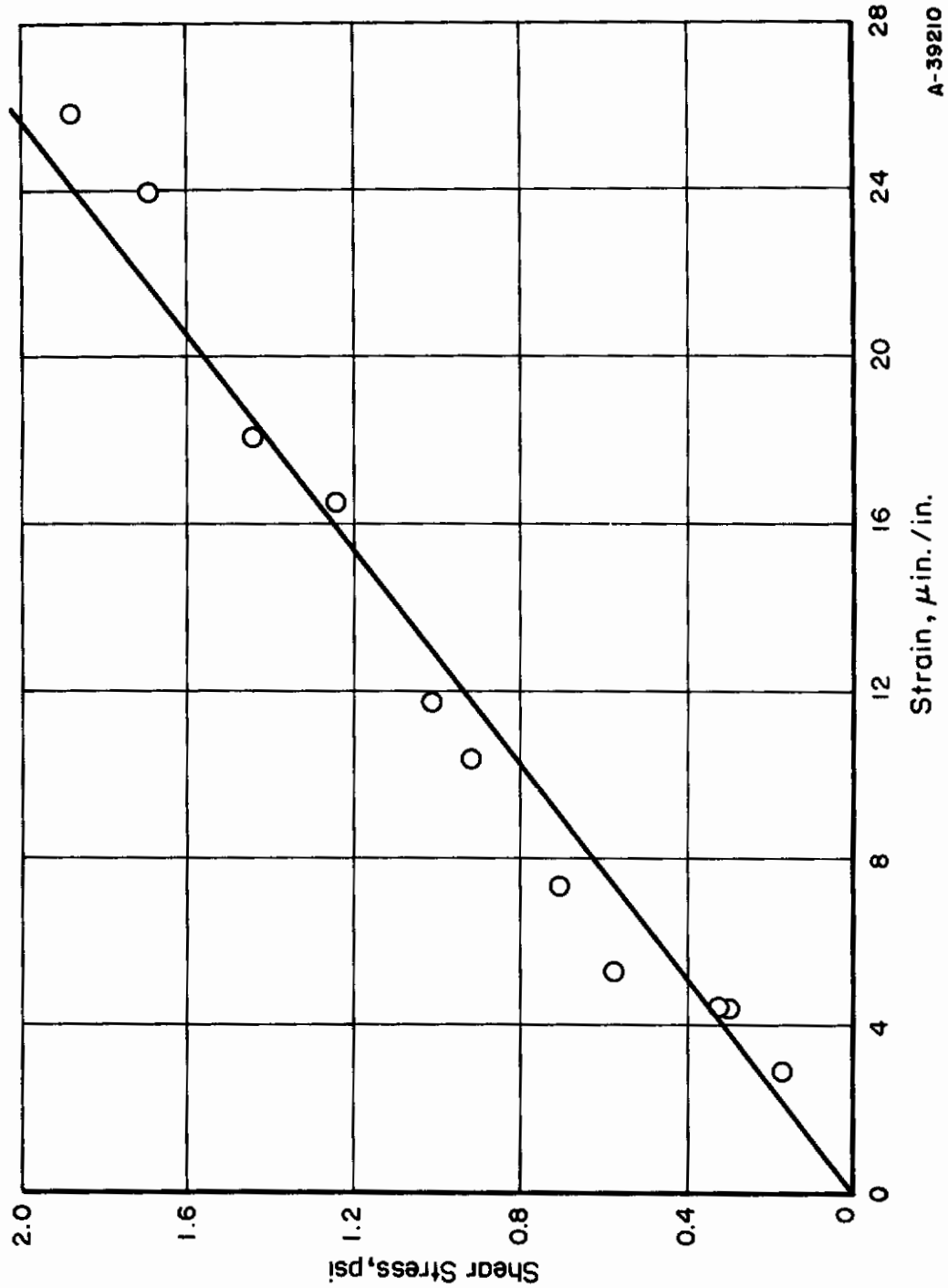

FIGURE 31. CALIBRATION OF PRESSURE TRANSDUCER SYSTEM

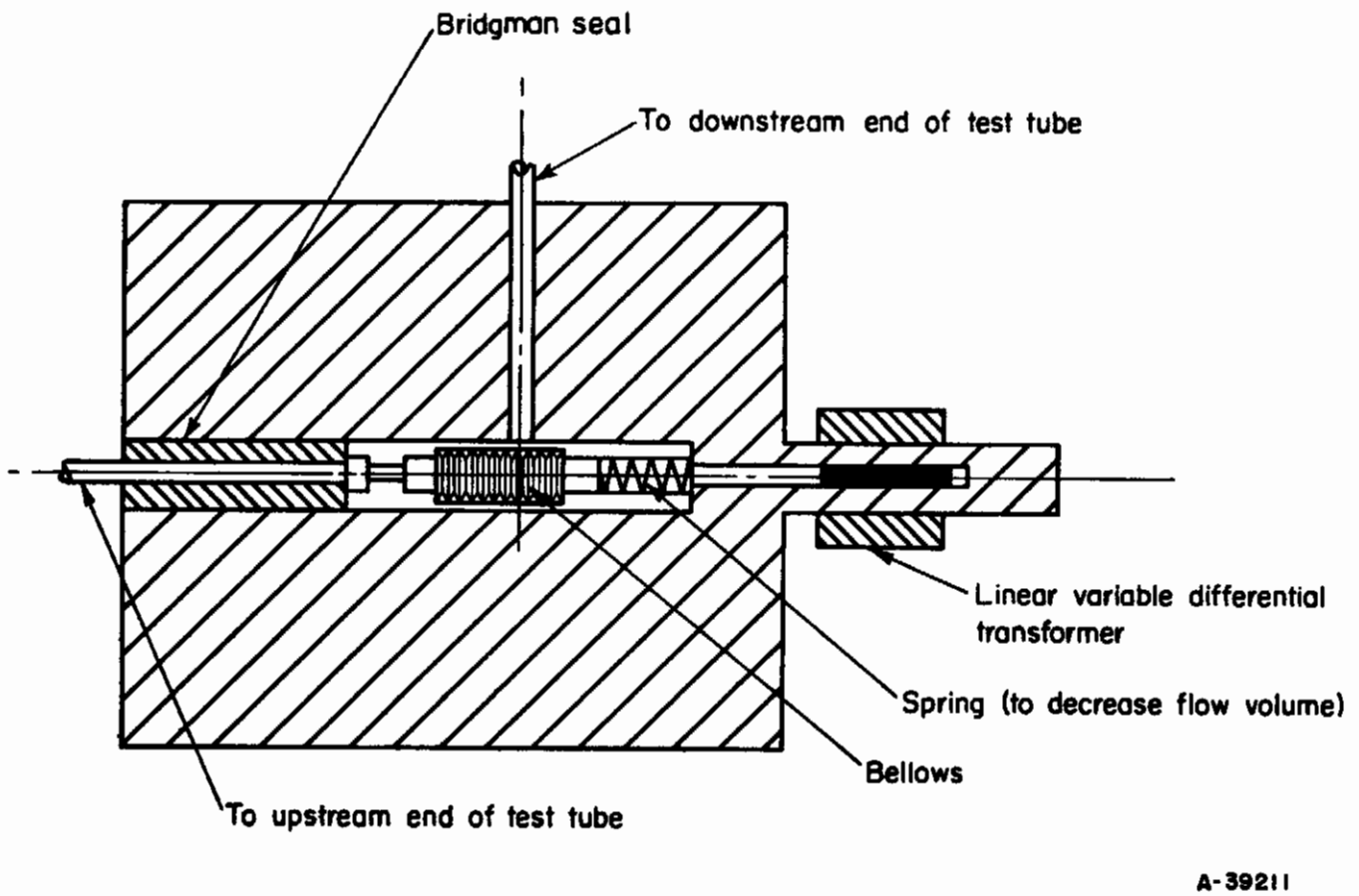

FIGURE 32. SCHEMATIC OF FLEXIBLE BELLOWS METHOD OF PRESSURE MEASUREMENT

The similarity of the above two film-thickness formulas obtained with quite different geometrical configurations is remarkable. Their similarity to the two theoretical formulas mentioned previously is also of interest. These formulas, derived for the elasto-hydrodynamic lubrication of infinitely long rolling cylinders with an isothermal incompressible Newtonian lubricant, are as follows:

Grubin:[9] $$\frac{h_o}{R} = 1.13 \left(\frac{P'}{E'R}\right)^{-0.091} \left(\frac{\mu_o \gamma V}{R}\right)^{0.727} ,$$

Dowson and Higginson:[10] $$\frac{h_o}{R} = 0.972 \left(\frac{P'}{E'R}\right)^{-0.13} \left(\frac{\mu_o V}{E'R}\right)^{0.7} (\gamma E')^{0.6} .$$

In the disk-machine experiments conducted over extended ranges of load, speed, viscosity, and temperature, however, new deviations of the film-thickness data from the above theory were evident. The negative exponent for the dependence of film thickness on load increased with increasing load, speed, and temperature. The dependence of film thickness on speed and viscosity seemed to decrease at high speeds and viscosities.

Most of the above effects of extended operating conditions on rolling-contact film-thickness relationships seem qualitatively related to temperature rise in the film which could be expected to decrease the effective film viscosity and, thus, film thickness. Increasing load, speed, and viscosity would be expected to increase viscous heating and thus the effect of temperature on film thickness. In fact, the elasto-hydrodynamic theory by Sternlicht, et al. [19], which accounts for such a film-temperature rise assuming adiabatic heating of the film, predicts a film thickness even less than those measured for the few numerical solutions available, as shown in Figure 10. However, the observed differences in minimum film thickness with lubricants having essentially the same viscosity coefficients and operating under the same conditions of load and speed (Figures 9 and 17) do not agree with the temperature-rise hypothesis. All other conditions being constant, the film thickness and the rounding of the contact shape were both more pronounced at high temperatures. Since the conductivity and the specific heat of oils tend to increase with temperature and the effect of temperature on viscosity decreases at high ambient temperatures, one would think that viscous heating in the film would tend to be less effective in reducing the film thickness at high ambient temperatures. The fact that just the opposite was shown in the experiments tends to discredit the temperature-rise theory as an explanation of the observed results.

Some clues as to a possible explanation of the observed deviations of the experimental data from isothermal Newtonian theory can be obtained by examination of the contact-deformation shapes shown in Figures 12 through 17. It will be noted that, in every case where the minimum film thickness

decreased considerably below the theoretical, the contact shape was more rounded than that for those profiles obtained under moderate conditions with a minimum film thickness near the theoretical. This trend in contact-deformation shape reflects a similar trend in the elasto-hydrodynamic pressure profiles generated in the lubricant films, since these film pressures cause the observed deformations. In particular, a more rounded contact shape indicates a pressure profile less like the Hertzian, which causes complete flattening of the contact. Rounded contacts indicate that the pressures are more spread out over the surface, especially at the edges of the contact region. This spreading of the pressure profile requires smaller pressure gradients in the lubricant and thus smaller lubricant shear stresses. It also implies that the lubricant film is being sheared over a larger area so that more lubricant has an opportunity to escape, leaving a smaller minimum film thickness, all other conditions being the same. If in fact the shear stress in lubricant films develops at a lessening rate with increasing shear rate at rolling contacts, as Smith has proposed[26], then it seems reasonable that this shear behavior, which is somewhat analogous to the yield stress in greases, will be more pronounced, corresponding to a lower yield stress, with increasing ambient temperature. Increasing load and speed subjects the lubricant film to more severe shear conditions and thus would also be expected to increase the effect of this lessening shear stress at high shear rates, i. e. , non-Newtonian behavior, in decreasing film thickness below that predicted by theories that allow no such nonlinear shear behavior, i. e. , Newtonian theories. In addition, these non-Newtonian effects should be more pronounced as the ambient viscosity is increased, which also agrees with the observed effects.

It is interesting to note in Figures 8 and 9 that the log-log plots of measured-film-thickness points versus load and viscosity coefficients, respectively, seemed to fall on fairly straight lines over distinct regions of operation with smooth transition curves between these regions. This behavior is analogous to the curves for the non-Newtonian elastohydrodynamic theory plotted in Figure 19, in which the curves for the highly non-Newtonian region are also linear with smooth transition curves into the Newtonian region. Film-thickness formulas for these theoretical curves in the non-Newtonian region are as follows.

$$\text{For } \frac{\gamma_2}{\gamma_1} = 0 : \frac{h_o}{R} = 3.0 \left(\frac{P'}{E'R}\right)^{-0.22} \left(\frac{\mu_o \gamma V}{R}\right)^{1.75} \left(\frac{4R}{\beta_o V}\right)^{1.41}$$

$$\text{For } \frac{\gamma_2}{\gamma_1} = \infty : \frac{h_o}{R} = 0.4 \left(\frac{P'}{E'R}\right)^{-0.31} \left(\frac{\mu_o \gamma V}{R}\right)^{2.50} \left(\frac{4R}{\beta_o V}\right)^{2.44}$$

It can be seen that this non-Newtonian theory predicts a considerably greater effect of load on the film thickness than that predicted by previously stated Newtonian theories. The negative exponent for load approaches the values determined by experiment even under moderate operating conditions in which some non-Newtonian effects may have existed. In addition, the effect of rolling speed on the film thickness is considerably less than that predicted in the Newtonian theory. The exponent for speed in the above equations varies from 0.34 for $\gamma_2/\gamma_1 = 0$ to 0.06 for $\gamma_2/\gamma_1 = \infty$. Although this exponent can become very small, it does not become negative under certain conditions, as found in the disk experiments. This and other discrepancies may be the result of assuming a Hertzian shape for the contact surfaces, which is probably more serious under non-Newtonian than under Newtonian conditions. However, this theory is satisfying in that it does correlate with the trends of the experiments.

Effect of Lubricants on Rolling-Contact Deformation and Stresses

If the non-Newtonian properties of lubricants in the inlet region of rolling contacts where the film thickness is generated are in fact important in these film-generation processes, then it would be expected that these properties would also have pronounced effects on the stresses in the rolling elements caused by the lubricant. It has already been shown how the contact-deformation shape in the direction transverse to the rolling becomes more rounded under the severe operating conditions at which non-Newtonian effects become pronounced. It is likely, therefore, that this rounding effect occurs also in the rolling direction. The sketch in Figure 33 shows the geometry and orientation of the rolling contact in the disk machine. The effect of the lubricant is presumed to be similar to that shown in the sketches of film pressures and deformations in Figure 34.

It will be noted in Figure 34 that the non-Newtonian behavior of the lubricant results in a thinner film at rolling contacts. In addition, the inlet region in which this film is generated is probably stretched out to a considerably greater extent than it is with a Newtonian lubricant. Because of this increased load support at the leading edge of the contact, the maximum pressure is probably reduced slightly below the Hertzian, or that which would occur if the surfaces were pressed together statically under the same load. In addition, the sharp pressure peak near the trailing edge of the contact, which is so in evidence in elasto-hydrodynamic theories which assume a Newtonian lubricant[15,17,19], is probably reduced in height and rounded off considerably with a reduced-shear-stress non-Newtonian lubricant.

The effect of the above apparent modifications in contact pressure and deformation profiles on the contact stress is illustrated by the estimates of

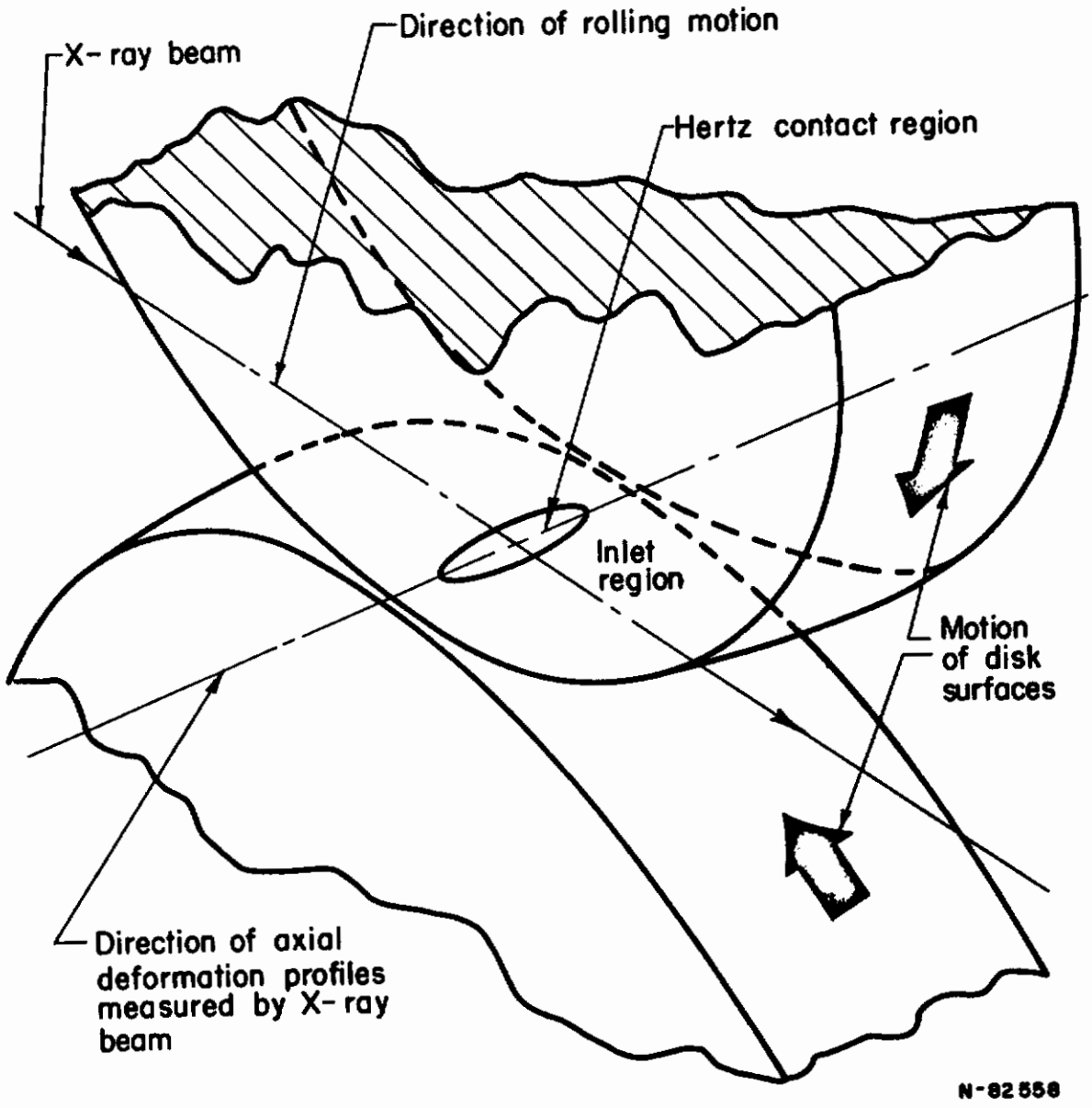

FIGURE 33. SKETCH OF ROLLING CONTACT IN DISK MACHINE

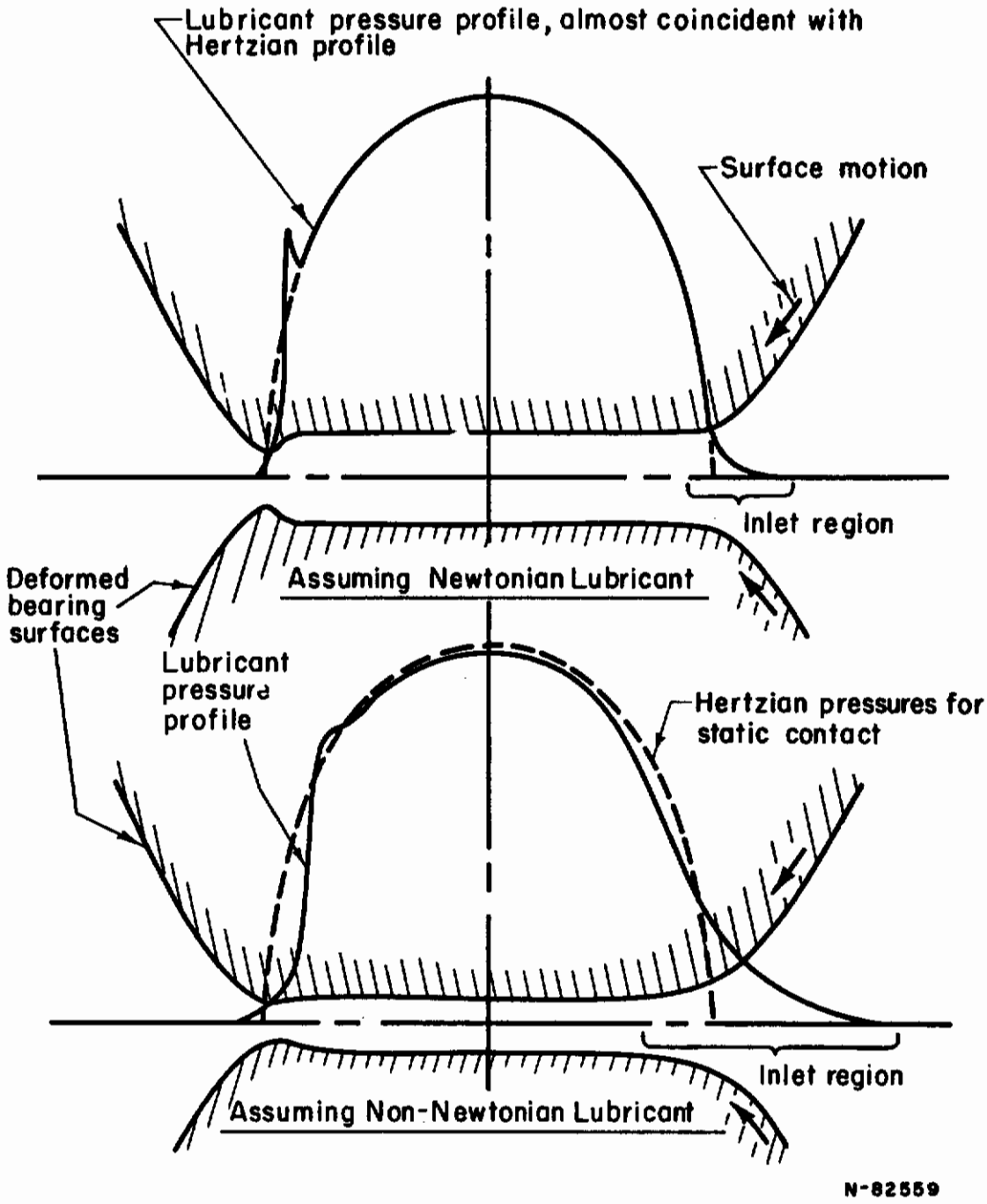

FIGURE 34. PROBABLE EFFECT OF NON-NEWTONIAN LUBRICANT BEHAVIOR ON DEFORMATION AND PRESSURE PROFILES AT ROLLING CONTACTS

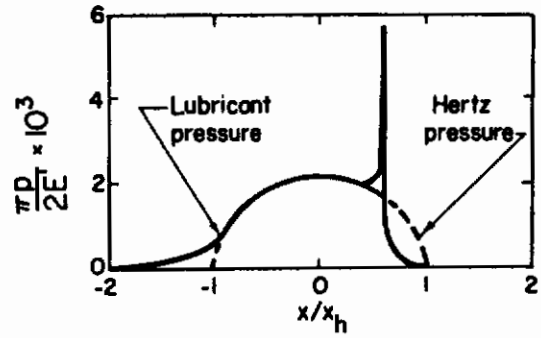

a. Lubricant Film Pressure

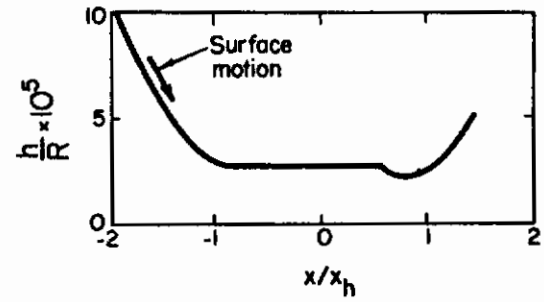

b. Lubricant Film Thickness and Contact Deformation

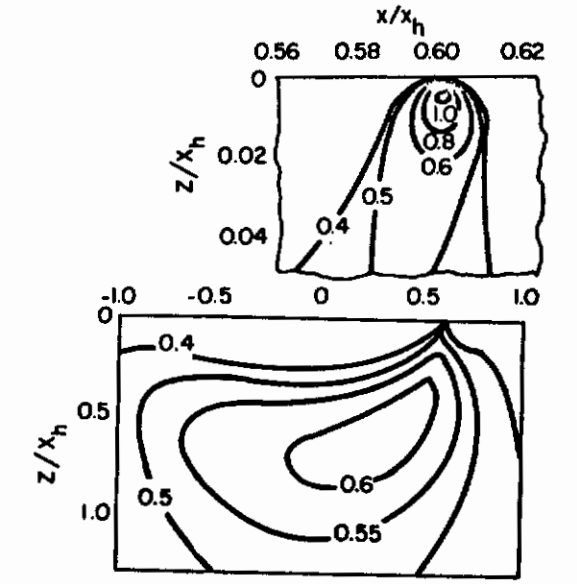

Contours of $\frac{\text{Maximum Principal Stress Difference}}{\text{Maximum Hertz Pressure}}$

N-82560

FIGURE 35. STRESSES AT ROLLING CONTACTS CAUSED BY THE LUBRICANT

Taken from Dowson and Higginson[16] for $\frac{P'}{E'R} = 1.9 \times 10^{-5}$ and $\frac{\mu_o \gamma V}{R} = 10^{-7}$.

ntact stresses for a lubricated rolling contact calculated by Dowson and igginson[16] and presented in Figure 35. The sharp pressure peak for the ewtonian lubricant assumed in Figure 35 results in a severe stress concentration slightly below the surface at the same position near the trailing dge of the contact. The maximum shear stress from this stress concentration caused by the lubricant in the rolling surfaces occurs at a point only a small fraction of the distance below the surface where the maximum Hertz shear stress occurs. It is interesting to note that the depth of the pits on rolling-contact surfaces caused by fatigue failure is usually about the same as the depth of the maximum shear stress (or more precisely, the depth of the maximum range of reversing orthogonal shear stress which Moyar[27] has found to correlate better with rolling-contact fatigue than the maximum shear stress). However, as Evans and Tourret found in their compilation of the depths of fatigue pits from several investigations[28], there are some instances of superficial pitting to depths much less than the depth of the maximum shear stress. If the stresses from the superficial stress concentration caused by the lubricant can actually cause fatigue failure of rolling elements, then the non-Newtonian properties of lubricants may have a marked effect on fatigue life under those operating conditions where the non-Newtonian behavior is significant.

FUTURE WORK

It is intended that further refinements will be incorporated into both the rolling-disk machine and in the high-pressure-lubricant rheology device to enable the more precise measurement and definition of those flow properties of lubricants that affect their performance at rolling contacts. Operation of the disk machine with lubricants having pure structures will be emphasized to explore the effect of structure on these properties and performance. Further development of lubrication theory at this time will probably be limited until more precise rheological data on lubricants are available. It is hoped that the present rheology machine can be developed to obtain such data, but other research methods will be considered as alternatives to the development of a practical understanding of the fundamental processes in rolling-contact-bearing lubrication.

REFERENCES

1. Sibley, L. B., Bell, J. C., Orcutt, F. K., et al., "A Study of the Influence of Lubricant Properties on the Performance of Aircraft Gas Turbine Engine Rolling-Contact Bearings", WADC Technical Report 58-565 (October, 1958), ASTIA No. 204218.

2. Sibley, L. B., and Bell, J. C., "Viscosity in the Lubrication Mechanisms of Rolling-Element Bearings", Symposium on the Role of Viscosity in Lubrication, ASME, New York (1960).

3. Sibley, L. B., Bell, J. C., Orcutt, F. K., and Allen, C. M., "A Study of the Influence of Lubricant Properties on the Performance of Aircraft Gas Turbine Engine Rolling-Contact Bearings", WADD Technical Report 60-189 (June, 1960).

4. Sibley, L. B., and Orcutt, F. K., "Elasto-Hydrodynamic Lubrication of Rolling-Contact Surfaces", ASLE Paper No. 61AM3B-2, to be published in ASLE Transactions (1961).

5. Crook, A. W., "The Lubrication of Rollers", Phil. Trans. Royal Soc. London A, 250 (981), 387-409 (1958).

6. Archard, J. F., and Kirk, M. T., "Lubrication at Point Contacts", Proc. Royal Soc. A, 261, 532-550 (1961).

7. Pressure-Viscosity Report, Vol. I and II, ASME Research Committee on Lubrication, ASME, New York (1953).

8. Private communication from Prof. J. A. Dixon, Pennsylvania State University, University Park, Pennsylvania.

9. Grubin, A. N., and Vinogradova, I. E., "Investigation of the Contact of Machine Components", Moscow, TsNIITMASh, Book No. 30, (1949), (D. S. I. R., London, Translation No. 337).

10. Dowson, D., and Higginson, G. R., "New Roller Bearing Lubrication Formula", Engineering, 192 (4972), 158-159 (August 4, 1961).

11. Crook, A. W., "Elasto-Hydrodynamic Lubrication of Rollers", Nature, 190 (4782), 1182-1183 (June 24, 1961).

12. Poritsky, H., "Lubrication of Gear Teeth, Including the Effect of Elastic Displacement", paper presented at the First ASLE National Symposium on Fundamentals of Friction and Lubrication in Engineering (September, 1952).

13. Dörr, J., "Schmiermitteldruck und Randverformung des Rollenlagers", Ingenieur Archiv, 22 (3), 171-193 (1954); see also "Theoretical Analysis of the Effect of Viscosity at High Pressure on Rolling Contact Bearings", Technical Status Reports No. 5 and 6 on Contract No. AF 61(052)-210 to Aeronautical Systems Division, USAF (1960).

14. Petrusevich, A., "Fundamental Conclusions from the Contact Hydrodynamic Theory of Lubrication", Izvest. Akad. Nauk SSSR, Otdel Tekh. Nauk (2), 209-223 (1951), (Ministry of Defense, London, Translation No. 293).

15. Dowson, D., and Higginson, G. R., "A Numerical Solution to the Elasto-Hydrodynamic Problem", J. Mech. Engrg. Science, 1 (1), 6-15 (1959).

16. Dowson, D., and Higginson, G. R., "The Effect of Material Properties on the Lubrication of Elastic Rollers", J. Mech. Engrg. Science, 2 (3), 188-194 (1960).

17. Archard, G. D., Gair, F. C., and Hirst, W., "The Elasto-Hydrodynamic Lubrication of Rollers", Proc. Roy. Soc., A, 262, 51-71 (1961).

18. Smith, F. W., "Lubricant Behavior in Concentrated Contact Systems – The Castor Oil-Steel System", Wear, 2, 250-263 (1958-59).

19. Sternlicht, B., Lewis, P., and Flynn, P., "Theory of Lubrication and Failure of Rolling Contacts", Trans. ASME, J. Basic Engrg., 213-226 (June, 1961).

20. Wolfe, R. J., and Berkson, W. G., "Report of Investigation of the Influence of Aircraft Gas-Turbine Lubricants on the Fatigue Life of Heavily Loaded Angular-Contact Ball Bearings", Final Report on Lab. Project 5912-1, Material Laboratory, New York Naval Shipyard (January 25, 1960).

21. Unpublished report on "Operation of Gas Turbine Mainshaft Bearings Under Conditions of Interrupted Lubricant Supply", to Allison Division of General Motors Corporation, Indianapolis, Indiana, from Battelle Memorial Institute on Purchase Order No. SE 77339 under Air Force Contract No. AF 33(600)-8786 (January 11, 1957).

22. Ree, T., and Eyring, H., "Theory of Non-Newtonian Flow. I. Solid Plastic System", and "Theory of Non-Newtonian Flow. II. Solution System of High Polymers", J. Appl. Phys., 26 (7), 793-800 (Part I) and 800-809 (Part II) (1955).

23. Hahn, S. J., Eyring, H., Higuchi, I., and Ree, T., "Flow Properties of Lubricating Oils Under Pressure", NLGI Spokesman, 121-128 (June, 1958).

24. Bell, J. C., "Lubrication of Rolling Surfaces by a Ree-Eyring Fluid", ASLE Paper No. 61LC-17, to be published in ASLE Transactions (1961).

25. Forster, E. O., "Relaxation Phenomena in Lubrication", Lubrication Engineering, 16 (11), 523-528 (1960).

26. Smith, F. W., "Lubricant Behavior in Concentrated Contact – Some Rheological Problems", ASLE Transactions, 3 (1), 18-25 (1960).

27. Moyar, G. J., "An Analysis of the Fatigue Strength of Surfaces in Rolling Contact", unpublished thesis written as partial fulfillment of requirements for M. S. degree, University of Illinois (1958).

28. Evans, L. S., and Tourret, R., "The Wear and Pitting of Bronze Disks Operated Under Simulated Warm-Gear Conditions", J. Inst. Petroleum, 38, 652-672 (1952).